AN INVESTIGATION OF AERODYNAMIC FORCE MODELLING FOR IMS RULE USING WIND TUNNEL TECHNIQUES

Fabio Fossati[1], fabio.fossati@polimi.it
Sara Muggiasca[2]
Ignazio Maria Viola[3]

ABSTRACT

Aim of this paper is to describe research activities carried out at Politecnico di Milano Twisted Flow Wind Tunnel with partial funding from the ORC in order to investigate the performance of upwind sails: in particular a series of rig planform variations in mainsail roach and jib overlap have been tested in order to overcome some perceived inequities in the ratings of boats of various rig design racing under the International Measurement System (IMS).The results of these investigation are used to assist the International Technical Committee (ITC) in changing the formulations in the IMS sail aerodynamic model.

1. INTRODUCTION

As well know the International Measurement System (IMS) is an handicap rule which provides elapsed time corrections for a broad range of sailing yacht types utilizing speed prediction from a velocity prediction program based on fundamental principles of hydrodynamics and aerodynamics: then the problem of properly modelling sail forces is a topic of the utmost importance.
The IMS Rule uses a Velocity Prediction Program (VPP) in which sail forces are represented by algorithms that are based on a combination of science and reverse engineering from the measured sailing performance of real boats.
Generally speaking in velocity prediction programs for yachts the problem of modelling sail forces is a fundamental focus. Two major topics have to be considered: several sailplan geometries must be taken into account and on the other side for given sailplan sails shapes are not fixed: alteration in sail trim produce a wide range of combination of lift, drag and heeling moment.
With reference to IMS VPP, the basis of IMS aerodynamic model is mainly derived from the aerodynamic model well known as Kerwin model.
Basically the IMS Rule does not measure sail shapes but sail size. The loads on each sail are found by multiplying the area of that sail by dynamic pressure and by the force coefficient for that kind of sail at the specified apparent wind angle. For each sail type there are curves of maximum lift and parasitic drag coefficient versus apparent wind angle. It is very important to point out that these coefficients do not represent the aerodynamic characteristics those sails would have if they were flying by themselves but when summed together the total force coefficients should accurately represent the aerodynamics of all the sails flying at any given apparent wind angle.
There are large fleets of boats successfully racing under the IMS Rule but from racing experience some inequities in the ratings of boats of various rig design sailing are perceived.

---

[1] Full Professor, PhD, Sailing Yacht Testing Scientific Coordinator CIRIVE – Wind Tunnel - Politecnico di Milano; Research Associate, ORC International Technical Committee
[2] PhD, CIRIVE – Wind Tunnel - Politecnico di Milano
[3] PhD student, Department of Mechanical Engineering, Politecnico di Milano

Aim of this paper is to describe research activities carried out at Politecnico di Milano Twisted Flow Wind Tunnel with partial funding from the ORC in order to investigate the performance of upwind sails: in particular a series of rig planform variations in mainsail roach and jib overlap have been tested in response to the above mentioned perceived inequities under the International Measurement System (IMS). The results of this investigation are used to assist the International Technical Committee (ITC) in changing the formulations in the IMS sail aerodynamic model. A large amount of work has been recently carried out by researchers [8] and more tests are planned in the next future in order to investigate also the fractionality effects on the planform aerodynamics.
This paper in the first part presents test arrangements, procedures and methodologies that have been carried out both for systematic gathering of wind tunnel data and subsequent analysis in order to describe aerodynamic behaviour of different sailplans.
Some interesting results and trends are presented and discussed.
Then a brief review of aerodynamic models available up to-date for VPP use is outlined; in particular an investigation of the methods of modelling the depowering of sails in VPP is considered.
Finally some basic ideas to provide a more suitable aero-model for upwind sails as required by IMS VPP to predict the performance of yacht for rating purposes are outlined. The new approach which is at the moment under ITC discussion is strongly based on the availability of an experimental data base according to the ITC research program guidelines.

2. POLITECNICO DI MILANO UPWIND TESTS PROGRAM

2.1. THE FACILITY

At the purpose of supporting with a state of the art facility the world-wide recognised excellence of Politecnico di Milano research in the field Wind Engineering as well as general Aerodynamics, Politecnico di Milano decided to design and build a new large Wind Tunnel having a very wide spectrum of applications and very high standards of flow quality and testing facilities. The Wind Tunnel is fully operative since September 2001 and in the first year of operations has been fully booked for applications in both fields of Wind Engineering and Aerospace applications.
Figure 1 shows an overview of the Wind Tunnel: it's a closed circuit facility in vertical arrangement having two test sections, a 4x4 high speed low turbulence and a 14x4 low speed boundary layer test section. The overall wind tunnel characteristics are summarised in Table 1. Peculiarity of the facility is the presence of two test sections of very different characteristics, offering a very wide spectrum of flow conditions from very low turbulence and high speed in the contracted 4x4m section (I_u<0.15% - V_{Matex}=55 m/s) to earth boundary layer simulation in the large wind engineering test section. Focusing on the boundary layer test section, its overall size of 36m length, 14m width and 4m height allows for very large scale wind engineering simulations, as well as for setting up scale models of very large structures including wide portions of the surrounding territory. The relevant height of the test section and its very large total area (4m, 56m^2) allows for very low blockage effects even if large models are included. The flow quality in smooth flow shows 1.5% along wind turbulence and ± 3% mean velocity oscillations in the measuring section. A very large 13m-diameter turntable lifted by air-film technology allows for fully automatic rotation of very large and heavy models fitted over it (max load 100.000 N).
The wind tunnel has a floating floor allowing for very clean model set-up, living all the instrumentation cable connections out of the flow. The very long upwind chamber is designed in order to develop a stable boundary layer and the flow conditions are very stable also in terms of temperature due to the presence of a heat exchanger linked in the general control loop of the facility. The Wind Tunnel is operated through an array of 14 axial fans organised in two rows of seven 2x2m independent cells. 14 independent inverters drive the fans allowing for continuous and independent control of the rotation speed of each fan. This fully computer controlled facility can help in easily obtaining, joined to the traditional spires & roughness technique, a very large range of

wind profiles simulating very different flow conditions and very different geometrical scales. The wind tunnel process is fully controlled by a PLC and a computer network (ABB control system), monitoring through more than 100 transducers all the most important flow parameters in terms of wind speeds, pressures, temperatures, humidity, vibrations of the fans and the structure, door opening etc., and allowing for feedback control on the flow temperature and speed. The flow conditions were found very stable and a confirm of that is the very low turbulence level in smooth flow. All the typical various set of spires have been developed in order to simulate the different wind profiles and an original facility has been recently installed allowing for active turbulence control in the low frequency range. Concerning the low-turbulence high-speed section, the large dimensions (4x4m) and the quite high wind speed (55 m/s) enable to reach quite high Reynolds numbers. Table 1 shows the very low levels of turbulence reached in this section, giving to the facility a very wide spectrum of possible applications. A very wide range of transducers, instrumentation and data acquisition systems are available allowing for all the typical boundary layer wind tunnel measuring applications in the wind-engineering field. More details on the facility can be found in [2] and [9].

Politecnico di Milano Wind Tunnel				
Tunnel Overall Dimensions			**50×15×15 $[m]$**	
Maximum Power (Fans only)			**1.5 $[MW]$**	
Test Section	Size $[m]$	Max Speed $[m/s]$	$\Delta U/U$ %	Turb. Int. I_u %
Boundary Layer	**14×4**	**16**	**< ±2**	<2
Low Turbulence	**4×4**	**55**	**< ±0.2**	< 0.2

Table 1: Overall wind tunnel characteristics

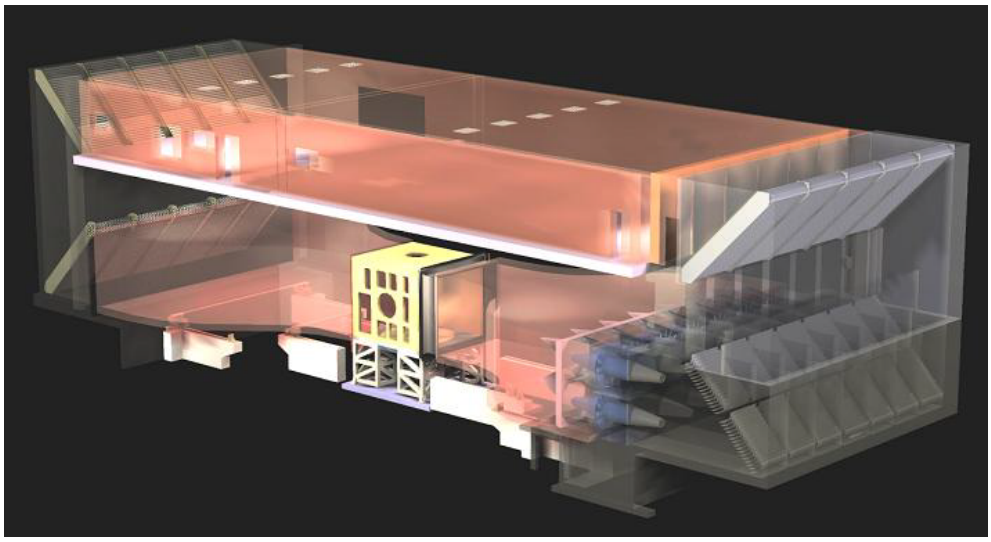

Figure 1: Politecnico di Milano Wind Tunnel 3D transparent rendering; the 14 2m diameter axial fans array is recognizable on the right lower side

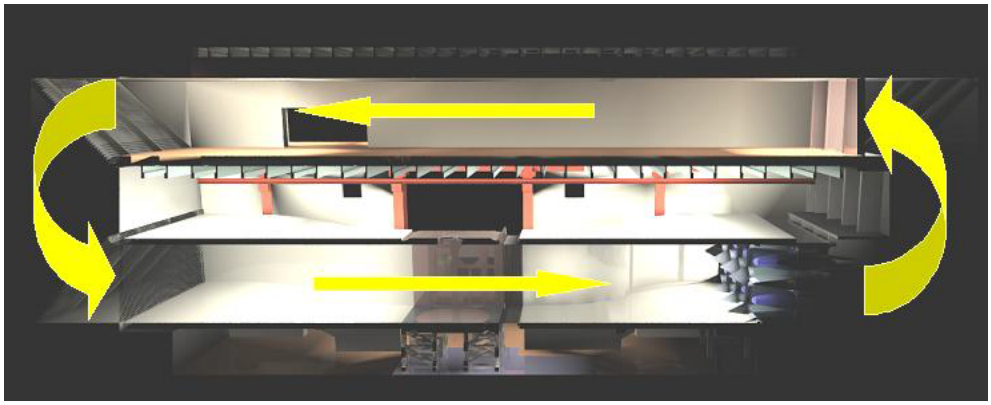

Figure 2: Longitudinal section showing the flow circuit; on the upper side is the boundary layer test section – on the lower side centre is the high speed low-turbulence test section – on the lower side at right is the 14 axial fans array

2.2. TEST ARRANGEMENTS AND MEASUREMENTS SETUP

A complete model, consisting of yacht hull body (above the waterline) with deck, mast, rigging and sails is mounted on a six component balance, which is fitted on the turntable of the wind tunnel. The turntable is automatically operated from the control room enabling a 360° range of headings.
The large size of the low speed test section enables yacht models of quite large size to be used, so that the sails are large enough to be made using normal sail making techniques, the model can be rigged using standard model yacht fittings and small dinghy fittings without the work becoming too small to handle, commercially available model yacht sheet winches can be used and, most important, deck layout can be reproduced around the sheet winch, allowing all the sails to be trimmed as in real life. Moreover the model yacht sheets winches are operated through a 7 channel proportional control system, by a console with a 7 multi-turn control knobs that allow winch drum positions to be recorded and re-established if necessary. The sheet trims are controlled by the sail trimmer who operates from the wind tunnel control room.
A high performance strain gage dynamic conditioning system is used for balance signal conditioning purposes.
The balance is placed inside the yacht hull in such a way that X axis is always aligned with the yacht longitudinal axis while the model can be heeled with respect to the balance.
Data acquisition can be performed in several ways: the usual procedure provides direct digital data acquisition by means of National Instruments Data Acquisition Boards (from 12 to 16 bits, from 8 differential channels up to 64 single ended) and suitably in-house written programs according to or Matlab standards.
The data acquisition software calculates the forces and moments using a calibration matrix. The forces are shown on the screen in real time so that the sail trim can be optimised. Actual measurements are obtained by sampling the data over a period specified by the test manager (generally 30 seconds) with a sample frequency specified too.
The raw data are stored in files that are used for the detailed data analysis.

2.3. SAIL PLANS TESTED

According to the overall activities program a series of sails was designed to investigate main girth and jib overlap. In particular 3 different main sails (with the same actual and IMS area but different roach) and 3 different jibs with different overlap were manufactured by North Sails Italia.
Politecnico di Milano CIRIVE Department provided a scale model of a sailing hull with mast and rigging. The dimension of the rig are as follows:

EHM		2.160 [m]
P		1.950 [m]
HBI		0.145 [m]
BAS		0.210 [m]
J		0.600 [m]
I		1.970 [m]
LPG	G100	0.580 [m]
LPG	G135	0.810 [m]
LPG	G150	0.900 [m]

Table 2

Table 3 shows different sails code with relevant roach and overlapping values

	Mims	Mhr	Mtri
Roach = MainAreaIMS/(1/2*P*E)-1	0.193	0.335	0.097

	G100	G135	G150
Overlap = LPG/J	1.00	1.35	1.5

Table 3:

The *"Mims"* code means that this mainsail girth is the maximum allowed by IMS Rule.
Considering the wind tunnel available time for testing only 5 different sets of upwind model sails have been tested.
In particular it was decided to test the 100% jib with all the 3 mainsails available and the IMS mainsail with the 135% and 150% overlap genoas.
Moreover all tests were performed in upright condition and at 30° heeling too.
Only the IMS mainsail+135% jib have been tested at 15° heeled condition too.
Apparent wind angles tested were chosen to be 22°, 27°, 32° and 42° in order to cover the upwind range.
Pictures of Figure 3 show model tested.

Mims G100

Mims G135

Mims G150

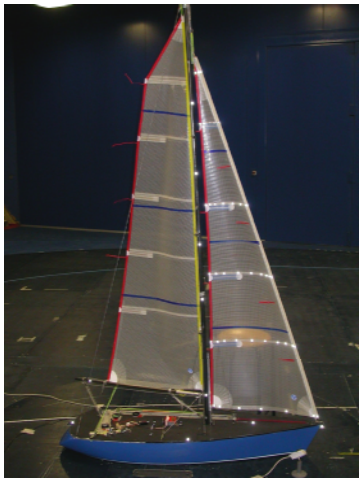

Mhr G100

Mtri G100

Figure 3

2.4. TESTING PROCEDURE

The yacht model is set at an apparent wind angle and at a fixed heel. After a sail trim has been explored, actual measurements are obtained by sampling the data over a period specified by the test manager (generally 30 seconds) with a sample frequency specified too.
The tunnel always runs at a constant dynamic pressure but, by trimming the sails in certain ways, the effect of different wind strength can be simulated.
An important feature of wind testing procedure is that the model should be easily visible during the tests so that the sail tell-tales can be seen by the sail trimmer. At this purposes four cameras are placed in the wind tunnel as well as onboard in order to help sails trimming procedure with sails view similar to the real life situation.
In particular a camera was placed on the floor looking at the yacht stern, another one was placed on the roof looking along the mast direction in order to check the mainsail flying shape, another one looks jib from deck and the last was used in order to control the genoa and jib car position.
The first task is to try to reach the maximum driving force consistent with light wind sailing. From there, the sails have to be either over trimmed, to get the part of the curve where stall is clearly evident, and sistemayically de-powered to collect data consistent with stronger wind conditions.
In Figure 4 a typical variation of the driving force coefficient Cx with heeling force coefficient Cy is reported.

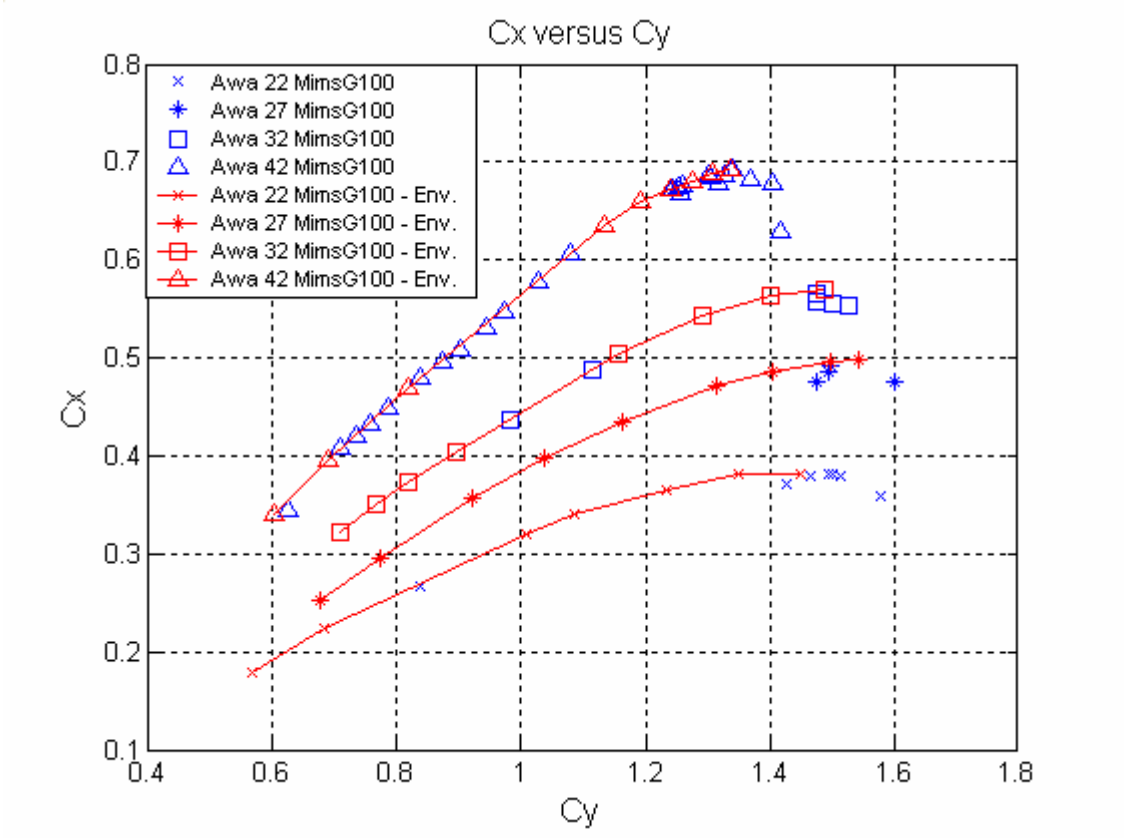

Figure 4

They are given by the expressions:

$$Cx = \frac{Fx}{\frac{1}{2}\rho S v^2} \tag{1}$$

$$Cy = \frac{Fy}{\frac{1}{2}\rho S v^2} \tag{2}$$

It can be seen that there are some settings at the highest values of heeling force coefficients where the driving force is lower than the maximum value. These non optimum values were obtained by oversheeting the sails such that the mainsail generally had a tight leech and the airflow separated in the head of the sail.

Envelope curves have been drawn through the test points with the greatest driving force at a given heeling force (Figure 4). In particular we are interested only on the envelope of all the sails trimming performed in order to exclude the non optimum sail setting position for the post processing which are non representative (see Figure 4).

Therefore a selection was made to choose those points that formed the envelope curves (maximum Cx for a given Cy value) for each apparent wind angle (Figure 4).

Trimming the sails to obtain optimum sailing points, i.e. points on the envelope curve proved to be the most challenging task of the test process. Attempts were made to carry out the job as systematically as possible. Firstly, the maximum drive point was found by trimming the sails to the best using the cameras views, the tufts on the sails and the force measurements output data.

From there, the heeling force would be reduced to simulate the trim of the sails for windier conditions: infact in windy conditions, to keep the optimum heeling angle, heeling force has to be reduced.

Once a specific trimming condition is obtained using the real time force and moments values displayed by the data acquisition system, a 30 seconds acquisition sampling has been performed with 100Hz sample frequency, and both time histories and mean values of each measured quantity can be stored in a file.

With reference to sails maximum camber configuration the decision was to adopt design camber values.
Some runs have been performed on the bare hull and rigging only (without sails) at different apparent wind angles to be able to evaluate windage. This has been subtracted from the measured data points in order to study the effect of the sail plan only.

2.5. DATA ANALYSIS PROCEDURE

The usual way of analysing data is to compare non dimensional coefficients, to be able to compare the efficiency of sails of different total area at different conditions of dynamic pressure.
The first analysis performed is the variation of driving force coefficient Cx with heeling force coefficient Cy as shown in Figure 4.
Also the plot of the Cx to Cy ratio versus Cy is very interesting. As an example with reference to the MimsG100 sail plan testing, Figure 5 shows a comparative plot of the Cx to Cy ratio versus Cy for the four apparent wind angles tested. Envelope curves have been drawn again through the test points with the greatest driving force at a given heeling force (Figure 4)

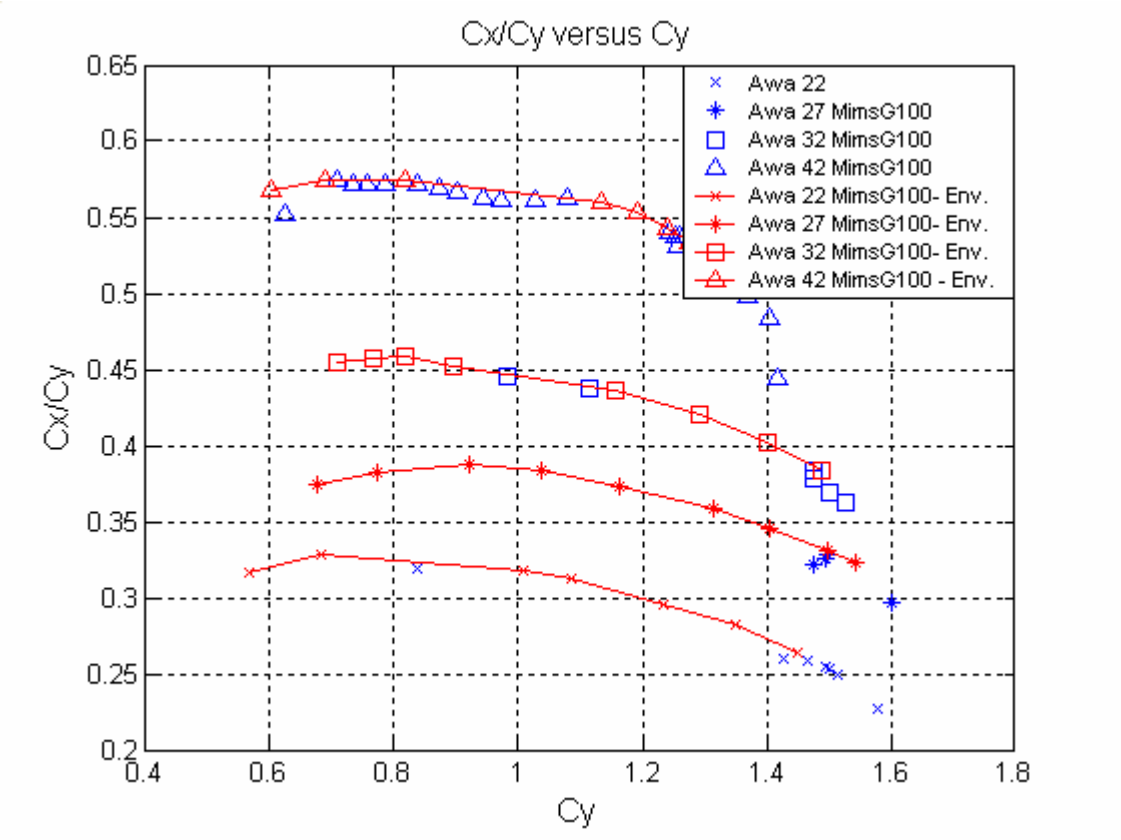

Figure 5

From the study of these plots some comments can be made:

- For a determined AWA and a given Cy the higher Cx, the more efficiently sail plan is operating
- For a given AWA the greatest efficiency of the sails is achieved when the Cx to Cy ratio is maximum
- From the comparison between the plots, it is observed that the max efficiency corresponds to a point with a lower driving force than the maximum. The translation of that in sailing performance terms is that, in light conditions when the maximum driving force is sought from the sails, there is some reduction in the rig efficiency that may be also affect boat speed. In medium wind, the sails are operating at their maximum efficiency. Finally in strong winds, where the sails are set to restrict the heeling force, the sail efficiency is reduced and some

reduction in the sail are may enable the sails o be re-sheeted to operate near the maximum efficiency.

- It is noted that for the same heeling force, the driving force increases with AWA. This reveals that it would be necessary to operate with the sails eased in order to sail with the rig at optimum efficiency at closer apparent wind angles
- Also Cx/Cy increases with AWA. When the yacht is sailing in steady conditions that ratio has to be matched by the resistance to side force ratio, therefore it is important to note that the more efficient hull will be able to sail closer to the wind.

The centre of effort height, Ceh, can be obtained by dividing the roll moment by the heeling force component in the yacht body reference system:

$$Ceh = \frac{Mx}{Fy} \tag{3}$$

As an example, a plot of its variation with heeling force for all angles can be seen in Figure 6. Both all the measured values and the envelope of the points corresponding to maximum driving force at each heeling force are reported. The results are given in terms of ratio between centre of effort height from boat deck and must length. For the purpose of the analysis only envelope curves through the test points with the greatest driving force at a given heeling force have been used.

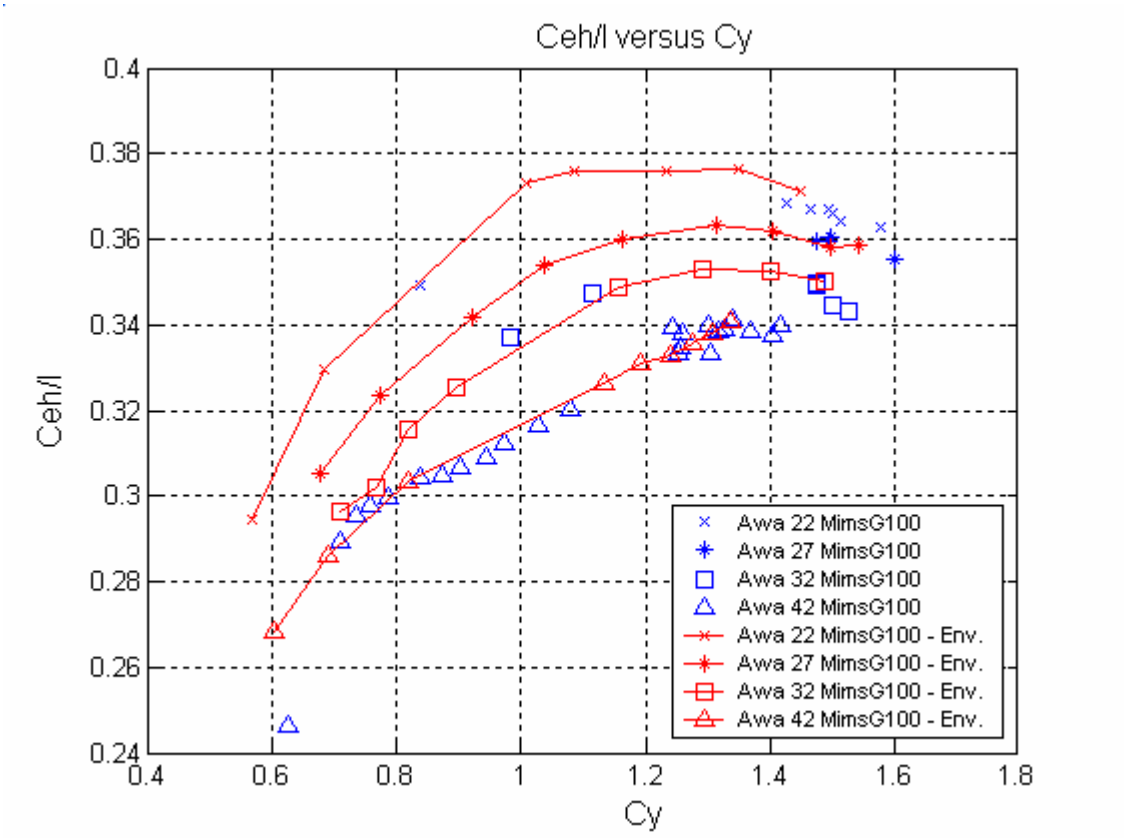

Figure 6

From the analysis of Figure 6 some comments are:

- The centre of effort height tends to reduce as the heeling force coefficients reduces. This is explained by the way in which the sails are de-powered to reduce Cy.
- The smaller the AWA is, the higher centre of effort is.
- The data show a quite big scatter due to the sensitivity of the Ceh to sail trim. Different trim position can have the same overall driving and heeling force but different Ceh because of a different span wise distribution of the forces.

The centre of effort longitudinal position, Cea, can obtained by dividing the yaw moment by the heeling force component in the yacht body reference system:

$$Cea = \frac{Mz}{Fy} \tag{4}$$

As an example, a plot of its variation with heeling force for all angles can be seen in Figure 7. Both all the measured values and the envelope of the points corresponding to maximum driving force at each heeling force are reported.

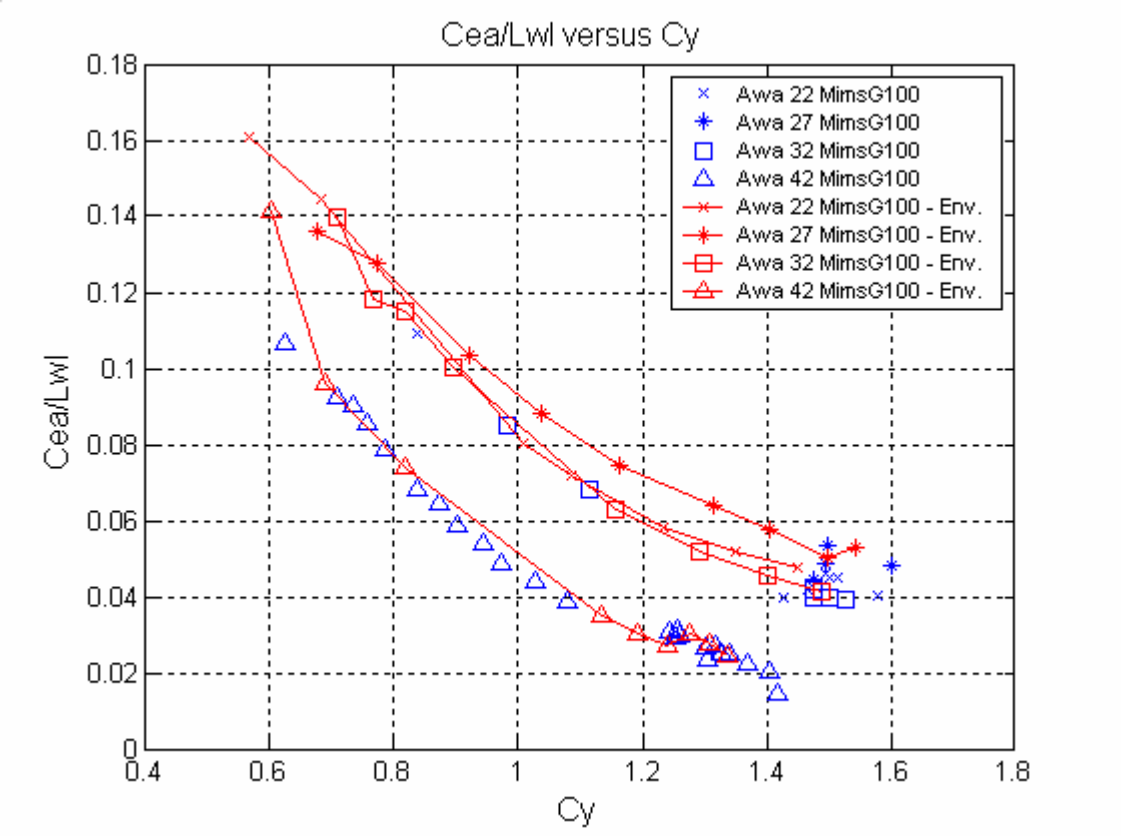

Figure 7

The results are given in terms of ratio between centre of effort longitudinal position from balance origin and yacht model length at waterline. Cea is measured from the origin of the balance which is placed behind the mast. It can be seen that Cea moves forward as Cy reduces. This is explained by the way the sails are de-powered.

Using the driving and heeling aerodynamic force Fx and Fy component in the yacht body reference system the corresponding drag and lift forces components can be obtained as follows:

$$DRAG = -F_x \cos(AWA) + F_y \sin(AWA) \tag{5}$$

$$LIFT = F_x \sin(AWA) + F_y \cos(AWA) \tag{6}$$

Then the corresponding drag and lift coefficients C_D and C_L can be evaluated:

$$DRAG = \frac{1}{2}\rho V_a^2 C_D(AWA) S \tag{7}$$

$$LIFT = \frac{1}{2}\rho V_a^2 C_L(AWA) S \tag{8}$$

The apparent wind speed V_a and apparent wind angle are evaluated in the heeled plane perpendicular to the mast according to:

$$V_a = \sqrt{\left(-V_t \cos\gamma\right)^2 + \left(V_t \sin\gamma \cos\phi\right)^2} \tag{9}$$

$$AWA = \text{arctg}\left(\frac{V_t \sin\gamma \cos\phi}{-V_t \cos\gamma}\right) \tag{10}$$

where γ represent the true wind angle (yaw angle), V_t is the wind tunnel flow velocity corresponding to the mean dynamic pressure at each run and ϕ is the heel angle.
As an example in Figure 8 and Figure 9 the C_D and C_L measured values at different AWA for MimsG100 upright test condition are reported. At each AWA, values corresponding to each run performed are reported and red full dots correspond to the maximum driving force condition trimming point.

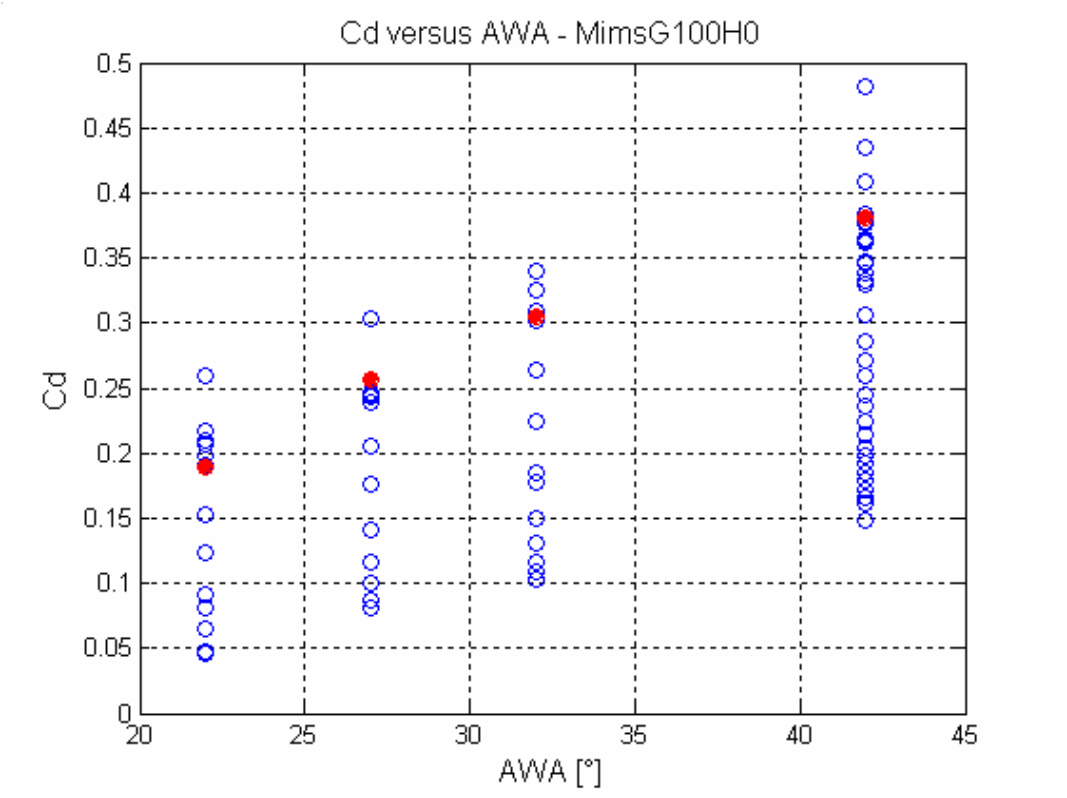

Figure 8

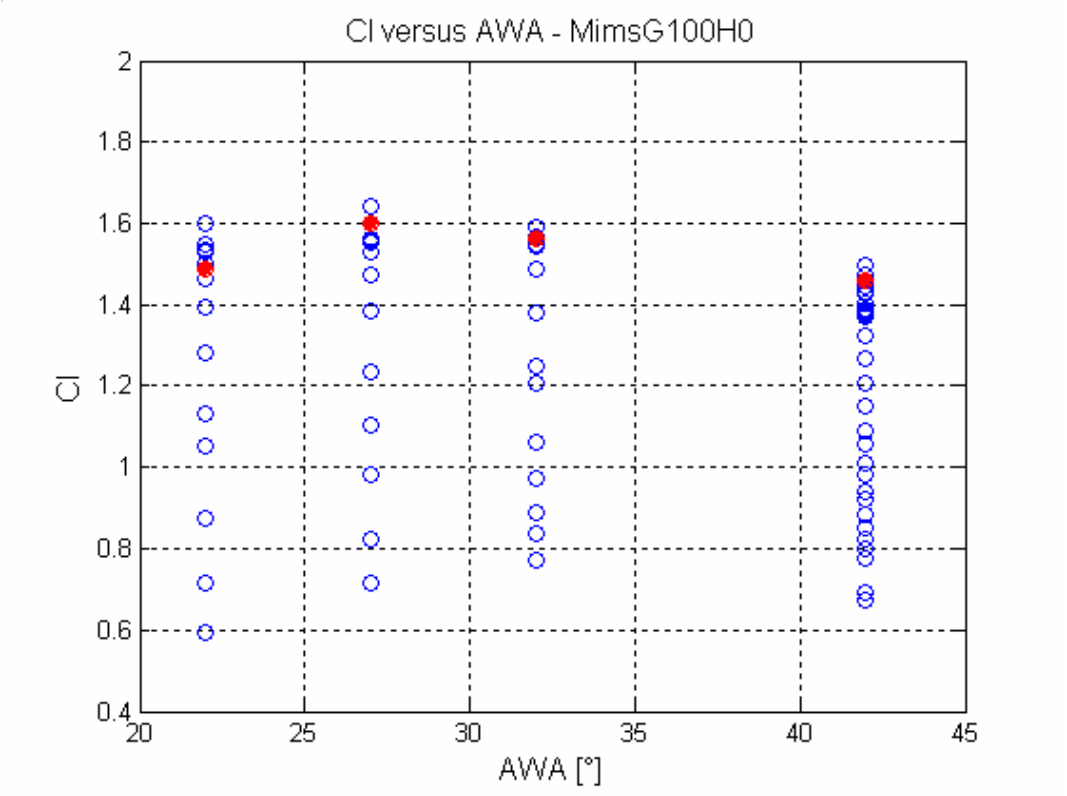

Figure 9

More information from the sail plan can be obtained from lift and drag coefficients because both the induced drag and quadratic profile drag vary with the square of lift.

By plotting the drag coefficients against lift coefficient squared the components of sail drag can be identified. That will be extremely informative and give the required input data for the current IMS VPP aero-model.

As an example in Figure 10 the drag coefficients against lift coefficient squared for each run performed at different AWA in upright condition is reported. Red line correspond to the maximum drive force condition trimming point envelope. As can be seen the envelope line fit points associated to the minimum drag at each lift produced by the sail plan.

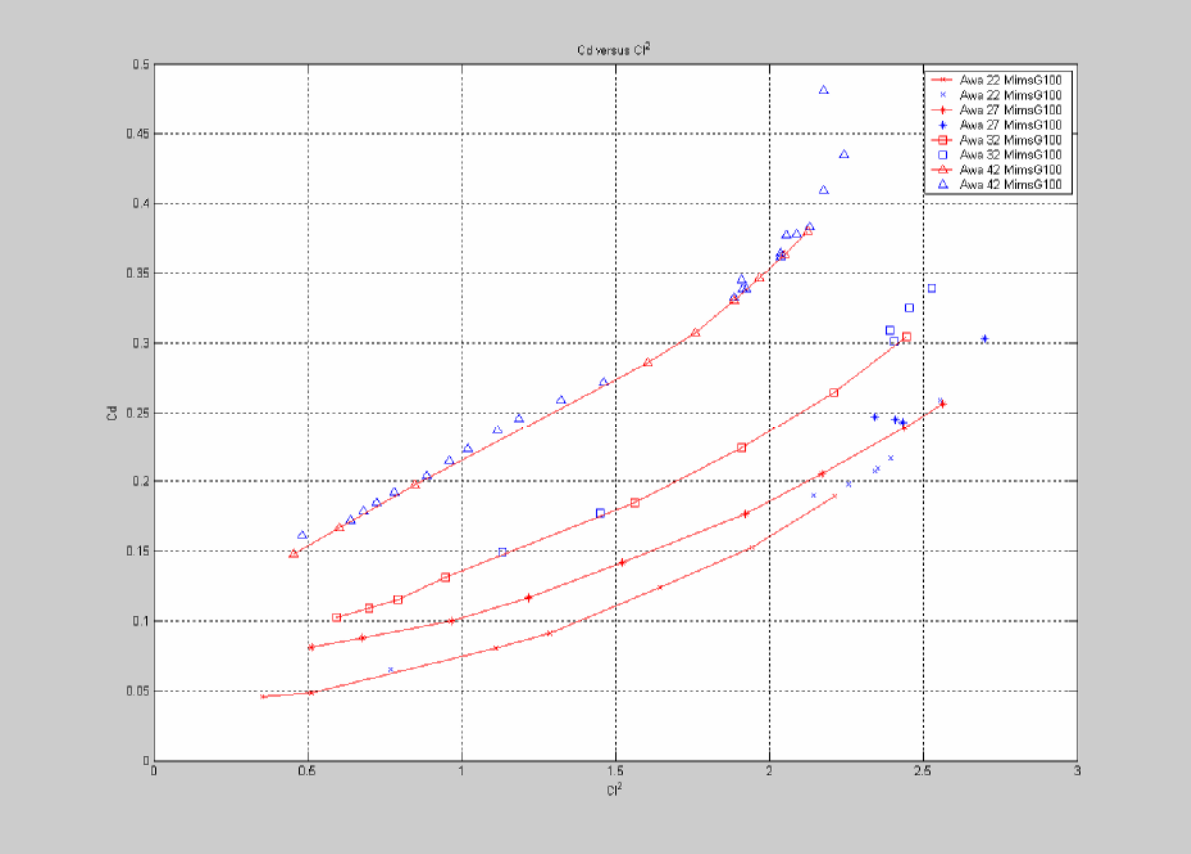

Figure 10

It is important to note that some data points within the low range of lift are above the induced line drag. This does not means that the testing accuracy is not good but that the sail setting of those points were not the optimum. For some reason the drag was higher than it could have been typically because there is some flow separation (in particular backwind on mainsail).
It can be seen that for lower values ofC_L^2 the data tend to collapse to a straight line, whereby C_D increases linearly with C_L^2.
This linear increase is attributable to the induced drag. The effective height Heff which is a measure of the efficiency of the rig can be determined from the slope of the straight line applying simple aerodynamic theory.
For higher values of C_L^2 the CD values increase more rapidly with C_L^2. This additional drag can be attributed to flow separation from the sails, particularly from the upper mainsail leech.
It can be seen that the intercept of the straight line with the zero lift axis through data from the lowest apparent wind angle is conveniently zero but at higher apparent wind angles there remains a residual base drag, not accounted for by windage which increases with the angle.
The intercept of the straight line with the zero lift axis directly represent the parasitic drag coefficient C_{DO} in the IMS model.
For each sail plan tested and for each AWA the effective height can be evaluated considering the linear regression between points that seem to be on a straight line: then the effective height is evaluated according to the following equation:

$$Heff = \sqrt{\frac{SailArea}{\pi Slope}} \tag{11}$$

As an example of this procedure see Figure 11.
Green line represent the linear best fit considering only 5 runs and the slope this straight line is used for effective height evaluation.

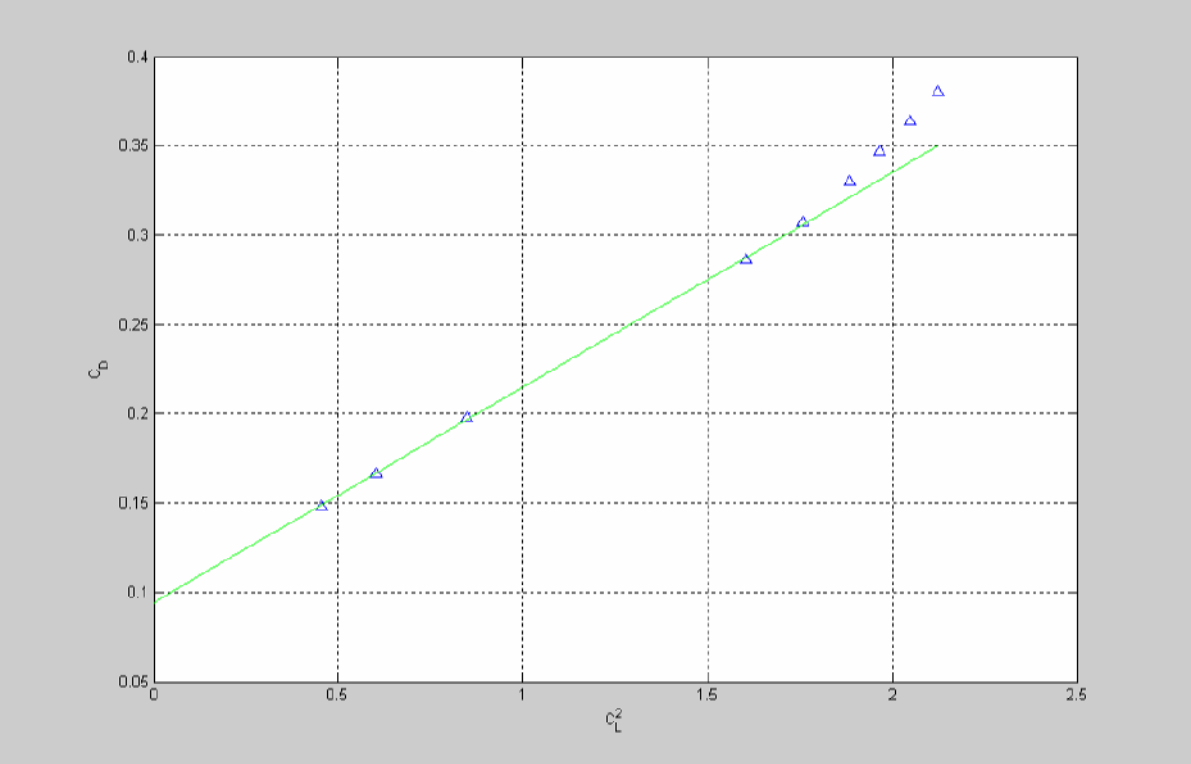

Figure 11

2.6. SOME RESULTS

In the following main results obtained in the upright condition are reported.
The relative performance of various rigs tested can be compared without recourse to full VPP calculations by comparing the driving force at similar apparent wind angle and heeling moments. A rig which produce a higher driving force for a given heeling moment, irrespective of the sail settings required to achieve this, will drive the yacht faster.
In Figure 12 the driving force area coefficient [m^2] versus heeling moment area coefficient [m^3] is reported for all the sail-plan considered at each of the AWA tested.
Different colours used refer to different sailplan (for instance blue corresponds to high roach main and 100% overlap jib) and different symbols are related to AWA.
It can be seen that genoas with overlapping have less induced drag (which is confirmed by the effective height as shown in the following) and produce a higher driving force for a given heeling moment.
At the same overlap IMS max roach seems to give better performance except at higher apparent wind angle tested.

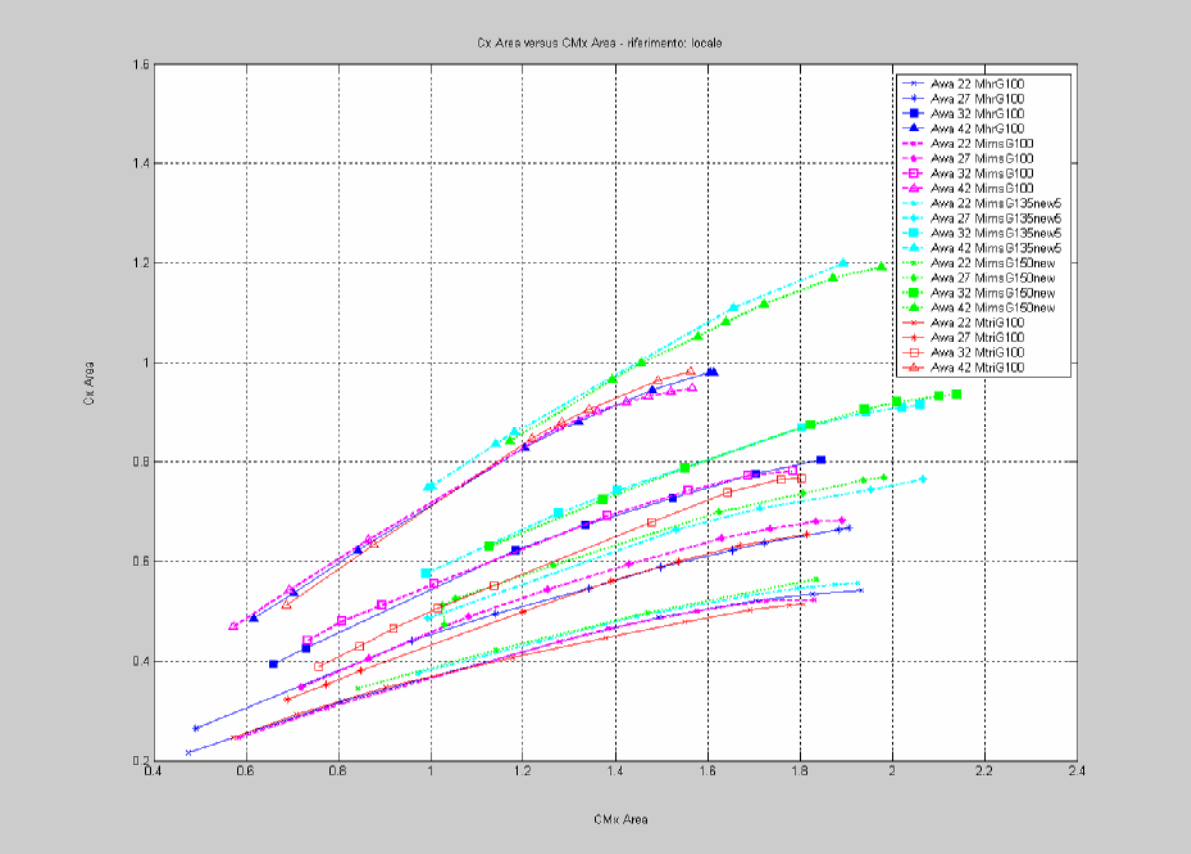

Figure 12

In Figure 13 the plot of the Cx to Cy ratio versus Cy is reported for all the sail-plan considered at each of the AWA tested.
Different colours used refer to different sail plan (for instance blue corresponds to high roach main and 100% overlap jib) and different symbols are related to AWA.

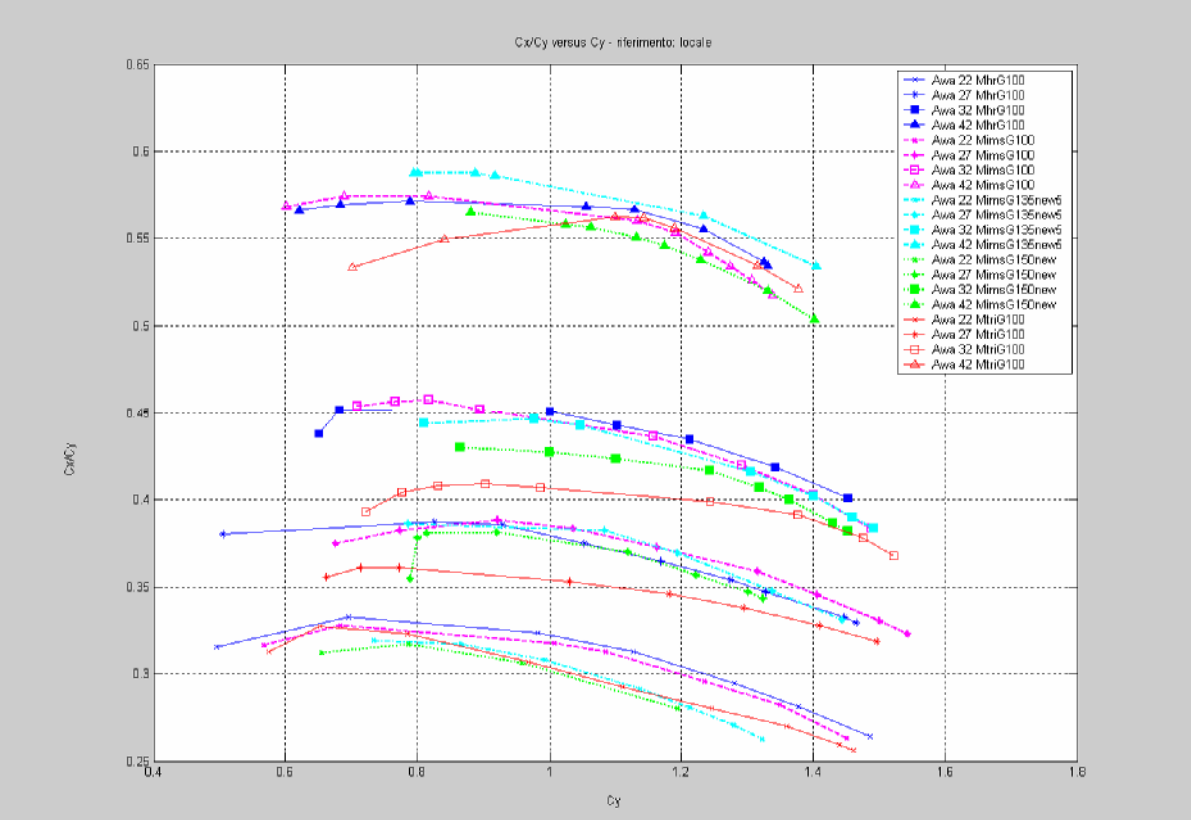

Figure 13

For a given AWA the greatest efficiency of the sails is achieved when the Cx to Cy ratio is maximum.
Mainsail roach gives better performance at each apparent wind angle tested (as confirmed by the effective height trend as shown in the following).
Figure 14 shows the centre of effort height above deck with respect to the mast height for different sail plan for the upright condition.
In particular for each sail plan the measured value at different AWA is reported and the relevant mean value (named "media") is reported too.

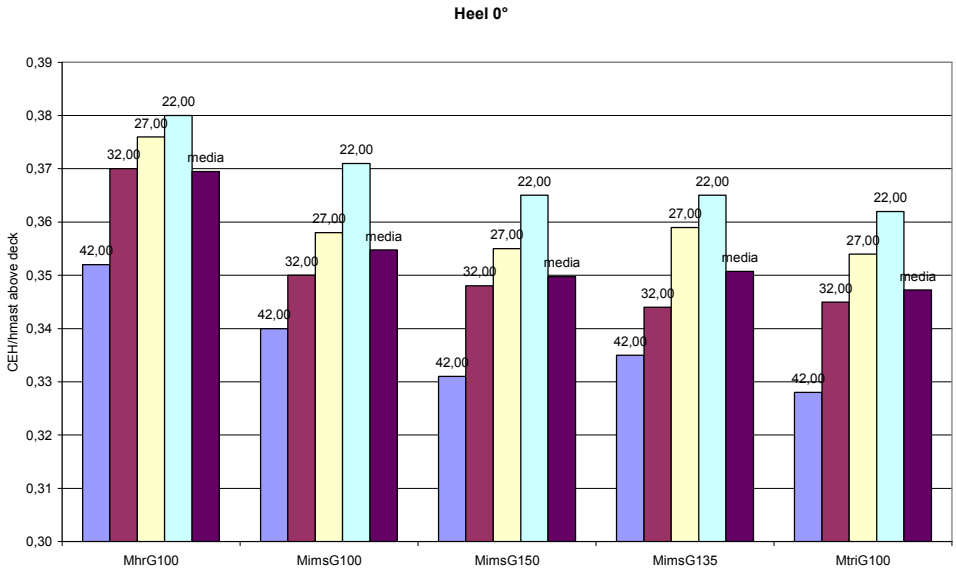

Figure 14

A number of comments can be made on the information given by this plot:

- The smaller the apparent wind angle is, the higher CEH is.
- Increasing mainsail roach (with the same overlap) CEH becomes higher.
- At the same mainsail roach, the smaller the overlap is, the higher CEH is. This is explained by the fact that increasing overlap sail plan has less area high up in the genoa.
- In any case this variation is quite inappreciable.

Following graphs summarise these comments.

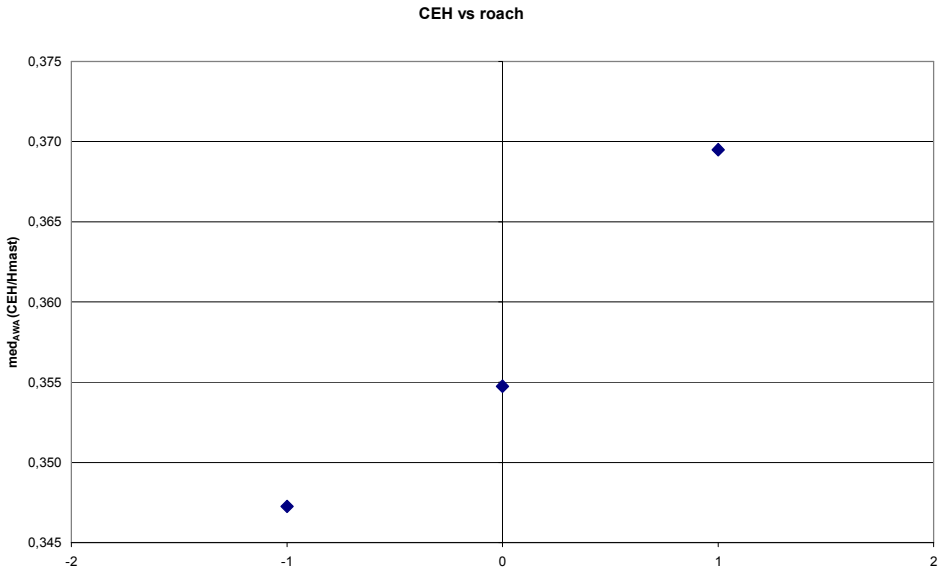

Figure 15

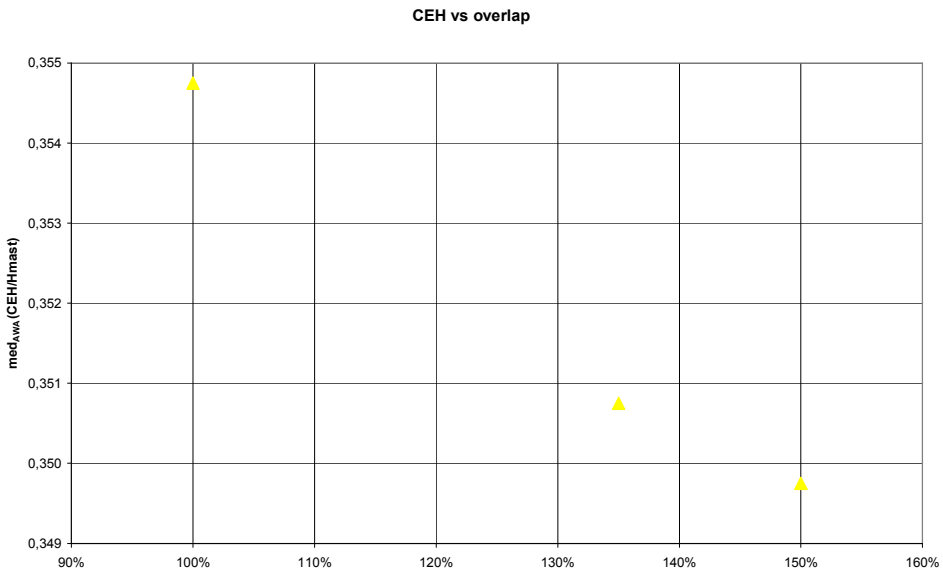

Figure 16

Figure 17 shows the ratio of the Effective rig height to the mast height for different sailplan in upright condition. In particular for each sail plan the evaluated effective height at different AWA is

reported and the relevant mean value for each sail plan is reported too. It can be seen that generally the effective height decreases with respect to the AWA.

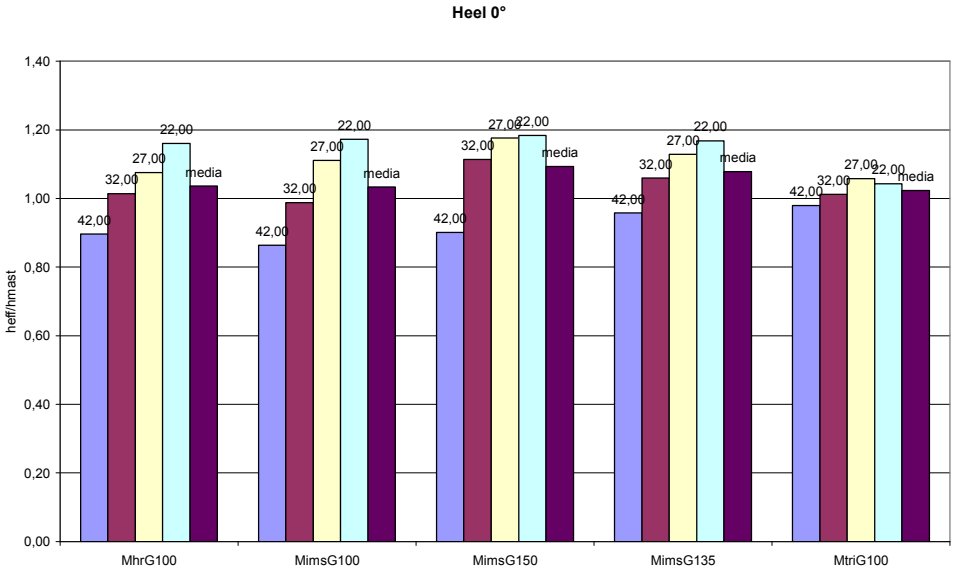

Figure 17

Following figure shows the change in effective rig height (mean value of different AWA results for each sail plan) with varying overlap.
The results show that there is a greater effective height, and less induced drag, with the jib overlapping increase.
In the same figure the Effective height for different mainsail roach is shown at the only available overlap (100%) for all of the mainsails tested.

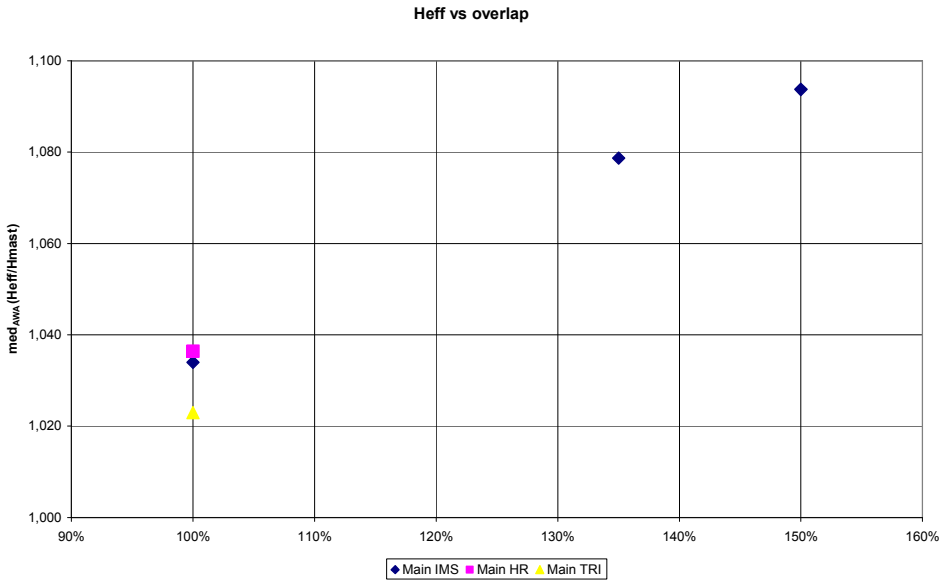

Figure 18

This roach effect is more detailed in Figure 19

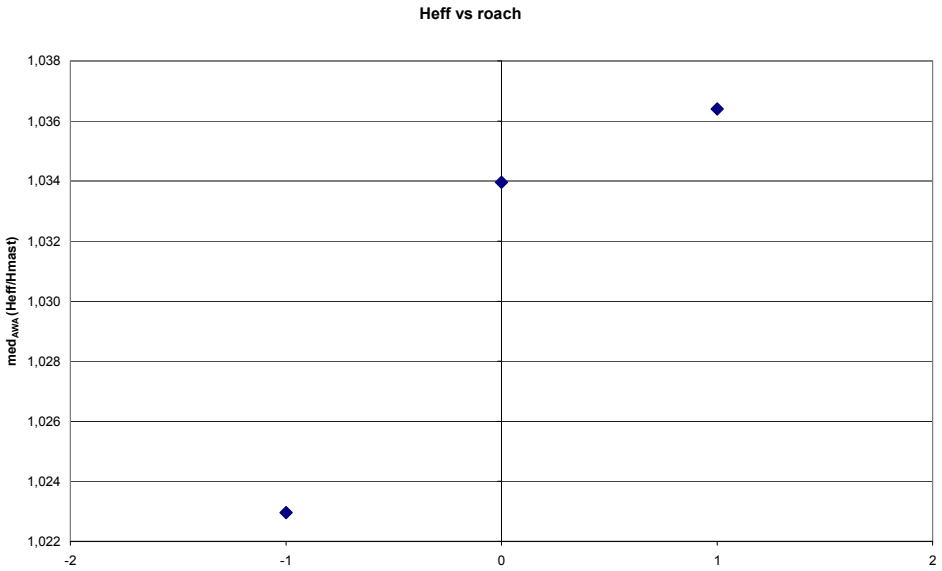

Figure 19

It seems to be some influence of roach but this should be more investigated also for other sailplan combination (i.e. with other jibs available). It should also be remembered that the calculation of effective rig height is very sensitive to variation in the data; in any case the obtained results have the same trend outlined in previous tests performed at the Wolfson Unit in 2002 [8].

GENERAL REVIEW OF AERODYNAMIC MODELS

In this paragraph a brief review of models for the aerodynamics of upwind sails available up to-date for VPP use is outlined with particular reference to the methods of modelling the depowering of sails.
Some remarks (based on the last ITC meetings discussions) on the current IMS aero model are summarised and a proposal for a new approach to model sail forces is outlined.
In velocity prediction programs suitable models must account for the effects of hull speed, heel angle, wind speed and direction and sail area and planform and shape. Generally this is accomplished by force and moments coefficients which provide aerodynamic and hydrodynamic forces and moments: the yacht performance may be predicted by solving the equilibrium equations.
More in details performance prediction requires a complete set of equation which is cabable of predicting the lift, drag and overturning moment of multiple interacting sails at any apparent wind angle and at any sail trim.
The principles of fluid dynamics require each of the various force coefficients (for instance with reference to lift produced by the sails)to depend on different factors as follows:

$$C_L = \frac{Lift}{qA} = C_L(AWA, heel, sailplan, shape) \tag{12}$$

where in particular

- *Sailplan* is the set of ratios describing sail shape which are fixed for a given set of sails

- *Shape* is the additional set needed to represent their flying shape, that is all of those changes which can be made by sail trimmers.

From a general point of view two different approaches can be used in order to manage the flying shape role in the above mentioned formulation which are basically devoted to find explicit expressions for the effects of these sail variables or to move from descriptions of sail shape to description of sail trim which may either explicit or implicit.
With particular reference to the former approach some workers have attempted to find explicit expressions for the effects of these sail variables directly by means of of incorporating CFD into design process and some other use direct methods making numerous CFD runs for various shapes of a given sail plan and feeding the results in the VPP [10], [11].
Within the limits of existing CFD and full scale or wind tunnel testing (at least up to date) it is most unlikely that the effects of every shape parameter on the force coefficients can be described with sufficient accuracy and even if it were possible, the sheer number of variables involved means that this approach is unlikely to find favour.
With reference to the subsequent approach based on explicit description of sails trim, it has the advantage of using variables which are readily measured in full scale or wind tunnel tests (like the position of mainsheet, jibsheet, traveller etc) but the disadvantage that they cannot easily be related to sail shape description.
Finally implicit measures of sail trim may be used which incorporate penalties for departing from an optimum sail setting, as embodied in the concept of reef and flat used in the Kerwin model and adopted currently in the IMS VPP.
The fundamental difference between this approach and the direct methods is that no attempt is made to explicitly link the aerodynamics of the sail with their shapes. In any case it is authors' view the only approach which is currently capable of realise a reasonable association between the parameters describing the shape of the sail and its corresponding aerodynamic performance is to use implicit measures of sails trim so extension to the current model will be suggested.

2.7. CURRENT IMS AERO-MODEL: SOME REMARKS

With reference to the current aerodynamic model of the IMS Rule a detailed description can be found in [5] and [8] provides thorough descriptions of subsequent aerodynamic model changes but essentially the basis of IMS aero model eqs is basically Kerwin model [2] (see also [12]):

$$C_L = flat * reef^2 C_{L\max}(AWA) \tag{13}$$

$$C_D = reef^2 (C_{D0}(AWA) + k * flat^2 C_{L\max}^2) \tag{14}$$

$$CEH = CEH(CEH_{geo}, flat) \tag{15}$$

$$k = kpp + \frac{1}{\pi Heff^2} \tag{16}$$

While the maximum lift CLmax the parasite drag CD_0 and the sailing centre of effort height CEH have to be supplied, this formulation cleverly avoids associating the sails forces with explicit features of sail trim and instead uses the reef and flat concepts to complete the system of equations for the force and moment balance.
The main topic of this approach is that sail shapes changes and their effects on aerodynamic properties are modelled using the well known reef and flat parameters.
In particular:

- Choosing flat<1 represents a deliberate reduction of lift in order to reduce the heeling moment or side force.
- Also the use of term flat indicates the reducing of sail camber would be one way of achieving this it is not necessary to say how this reduction is actually achieved in practice.
- Similarly the factor reef multiplies the sail size so that reef<1 represents the reduction on moment by a reduction of sail area (reefing) and consequent lowering the centre of effort and induced drag.

For a given apparent wind angle (AWA) the VPP chooses values of *reef* and *flat* to maximise yacht performance.
To have survived so long this model must *obviously work well*, which is interesting because looking at this model some obvious deficiencies are revealed: in particular first it is important to note that reef is a *geometric* rather than an *aerodynamic factor* (if the actual sail area is used to form the coefficients the reef factor would not appear). In addition we know that when the set of sails are trimmed to their optimum aerodynamic state (elliptic or semi-elliptic loading) but the resulting overturning moment is too great, then the optimum loading now becomes that which minimise drag for a given lift and for a given heeling moment. In this condition the corresponding induced drag must be greater than that of an unconstrained moment, that is as the centre of effort of sails is trimmed further away from the aerodynamic optimum at fixed lift, the induced drag must increase. This is not correctly modelled using reef since eqn 1b always has the drag reducing with the centre of effort.

2.8. THE JACKSON AERO-MODEL: SOME REMARKS

In order to overcome the above mentioned problems Jackson (1998) introduced a new parameter called *twist* which explicitly models the relationship between *Induced Drag*, *Lift* and *Centre of Effort Height*
Basic equation of Jackson model are the following:

$$C_L = C_{L\max}(AWA) \tag{17}$$

$$C_D = C_{D0}(AWA) + k * C_L^2 * (1 + ct^2) \tag{18}$$

$$t = 1 - \frac{Ceh}{Ceh_{opt}} \tag{19}$$

$$k = kpp + \frac{1}{\pi Heff^2} \tag{20}$$

$$Ceh = Ceh_{opt} * (1 - t) \tag{21}$$

where:

- t is called twist parameter
- t is zero when the centre of effort is at its optimum height Ceh_{opt}
- t^2 gives the required penalty in induced drag for not keeping the centre of effort height at the height corresponding to semi-elliptic loading
- c is the twist weight function

C_{D0}, Ceh_{opt} and k value can be obtained from experimental results fitting available drag and centre of effort data to the expression (eq.18).
As an example, Figure shows a scatter plot of the predicted versus actual drag for IMS mainsail and 100% overlapping jib.
Ideally this will result in a plot with all the data on a 1:1 straight line, but the onset of separation cause data to diverge.
This unsuccessfully behaviour has been generally found considering also experimental data available from other sailplan tested: then a new approach, strongly based on the availability of an experimental data base according to the ITC research program guidelines will be outlined in the following.

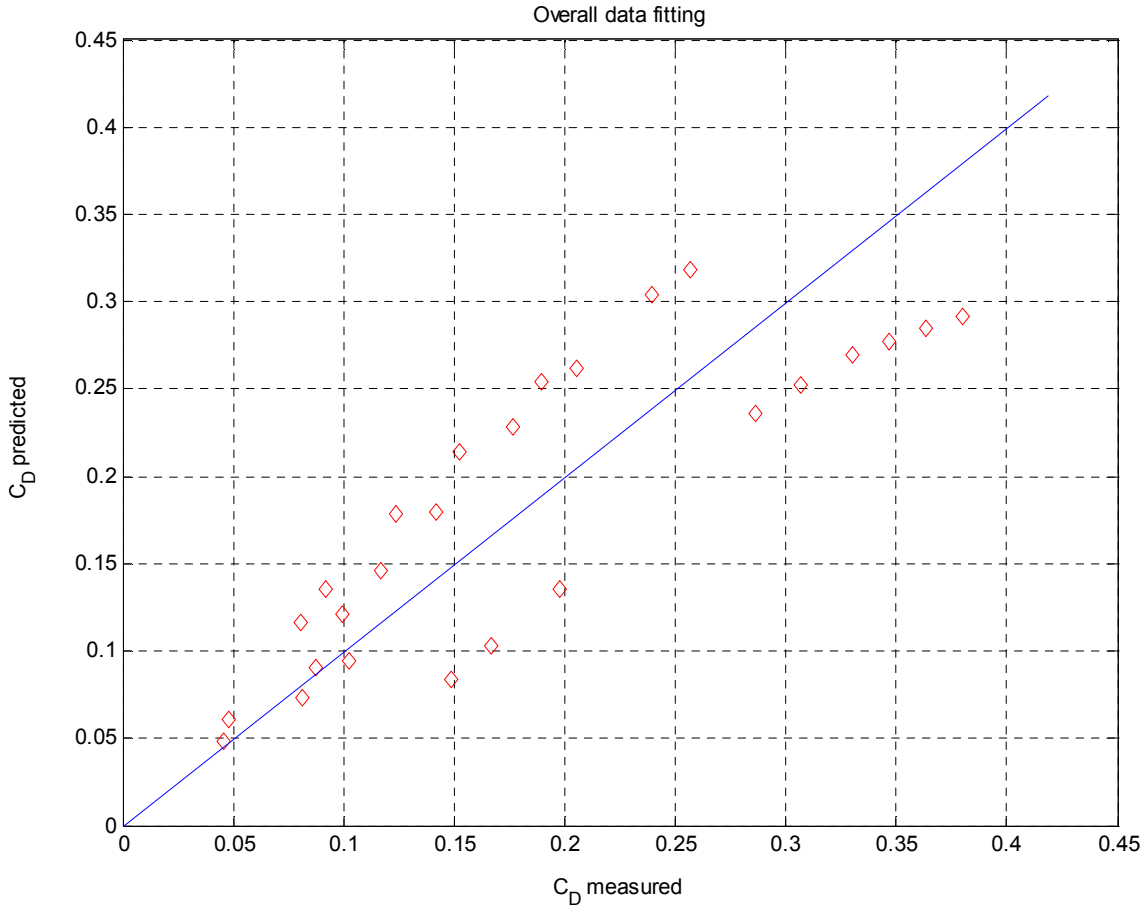

Figure 20

3. SOME BASIC IDEAS FOR A NEW UPWIND AERO-MODEL

With particular reference to the current IMS VPP aero-model, it should be also noted that some other obvious deficiencies are revealed. In particular:

- Once sailplan is decided, sail area changes occur in discrete steps and not necessarily by scaling all sails dimensions equally (see various headsail codes).

- Both overlap and roach (i.e. sail plan geometry) seem to affect effective height and aerodynamic coefficients

From tests results it seems that different C_D and C_L curve with respect to AWA could be considered for different sail plan. In the current IMS aero model this is accomplished by combining the individual sail's characteristics to produce a set of lift and drag coefficients that describe the aerodynamic behavior of the entire rig [5]. The drawback of this approach is that mainsail roach does not affect the sail plan aero coefficients. As an example Figure shows a comparison between experimental data and current IMS aero-model Drag and Lift predicted values for different main roach + non overlapping jib.
In Figure the comparison in terms of effective height is reported too.

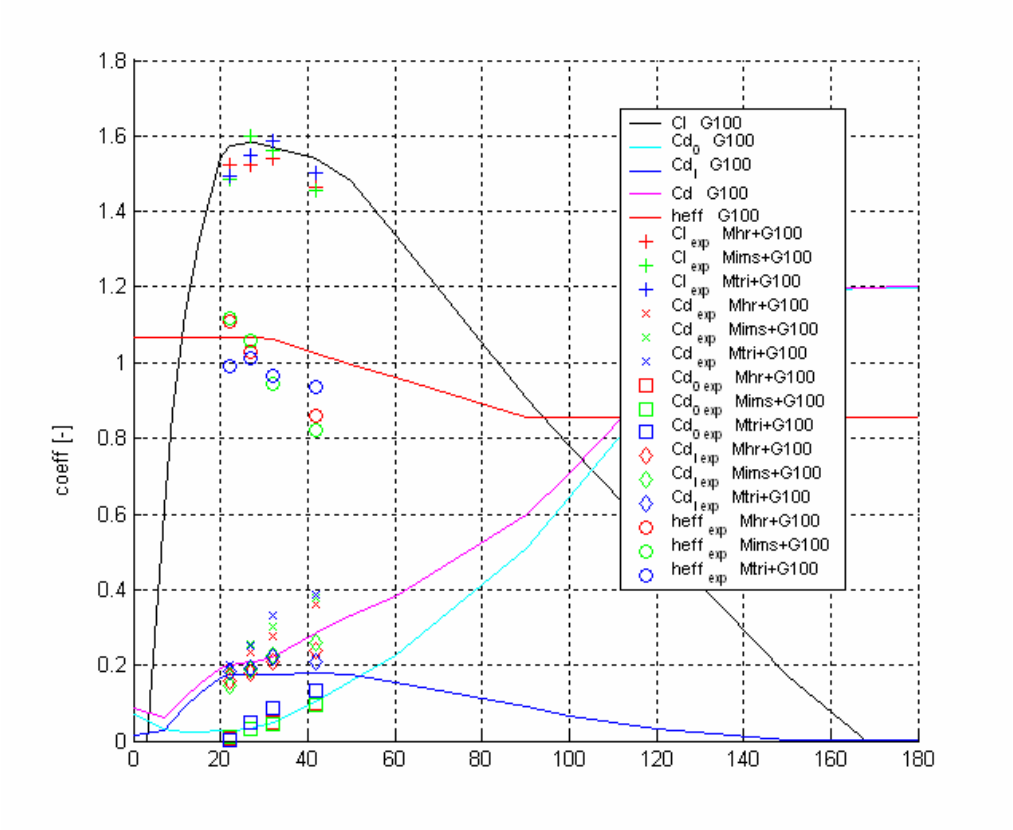

Figure 21

Figure shows the comparison between experimental data and current IMS aero-model predicted values for sailplans with different overlap and the same mainsail.

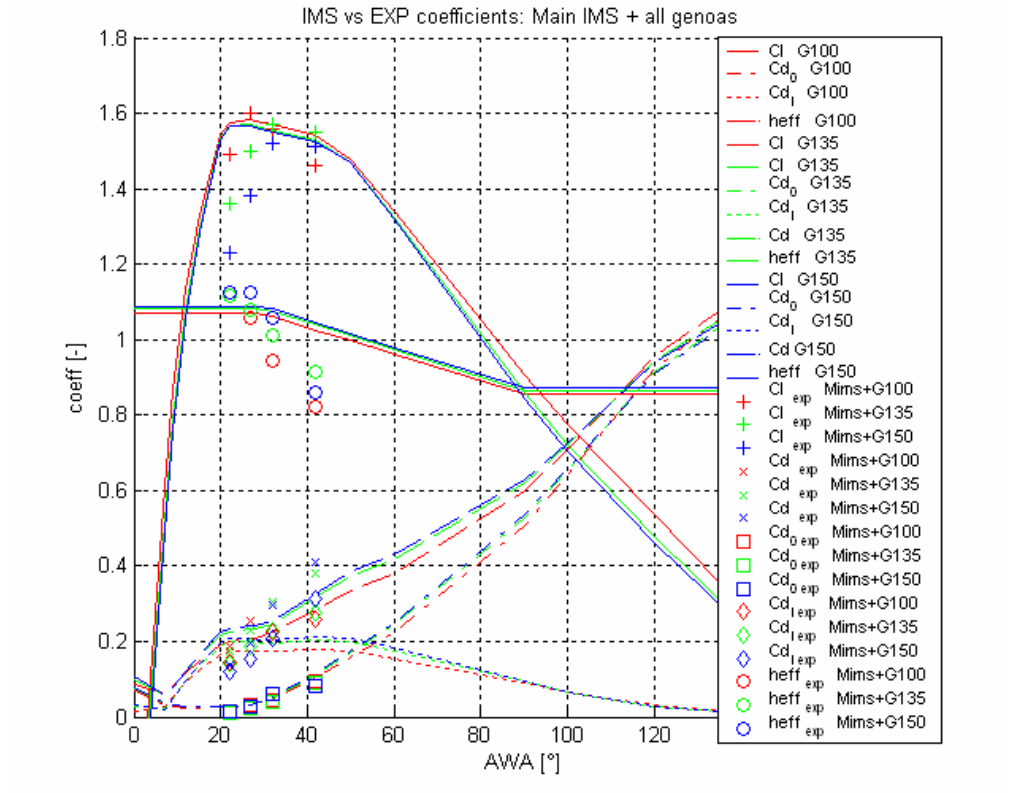

Figure 22

In this case great difference in terms of CL coefficients predicted by actual IMS formulation with larger overlapping at typical close hauled apparent wind angles is pointed out. This means in particular that boats with overlap are supposed faster than they are.
Taking into account that the CL max is directly obtained from the experimental measures and that it is simply an IMS VPP input, different coefficients sets should be considered for different overlapping sailplans.
Also the total drag of overlapping sails at typical close hauled apparent wind angles is under estimated too.
Moreover considering a typical C_D vs C_L^2 plot obtained from tests (Figure) emerged that:

- generally the maximum drive condition may be associated with some separated flow.
- effective height seems to be strongly dependent on apparent wind angle
- taking into account the (C_{Lmax}(AWA) and $C_{Dmaxdrive}$(AWA)) curve the actual decline of C_D, as C_{Lmax} is reduced, would follow the straight dotted line which means have a drag value higher than it should be.

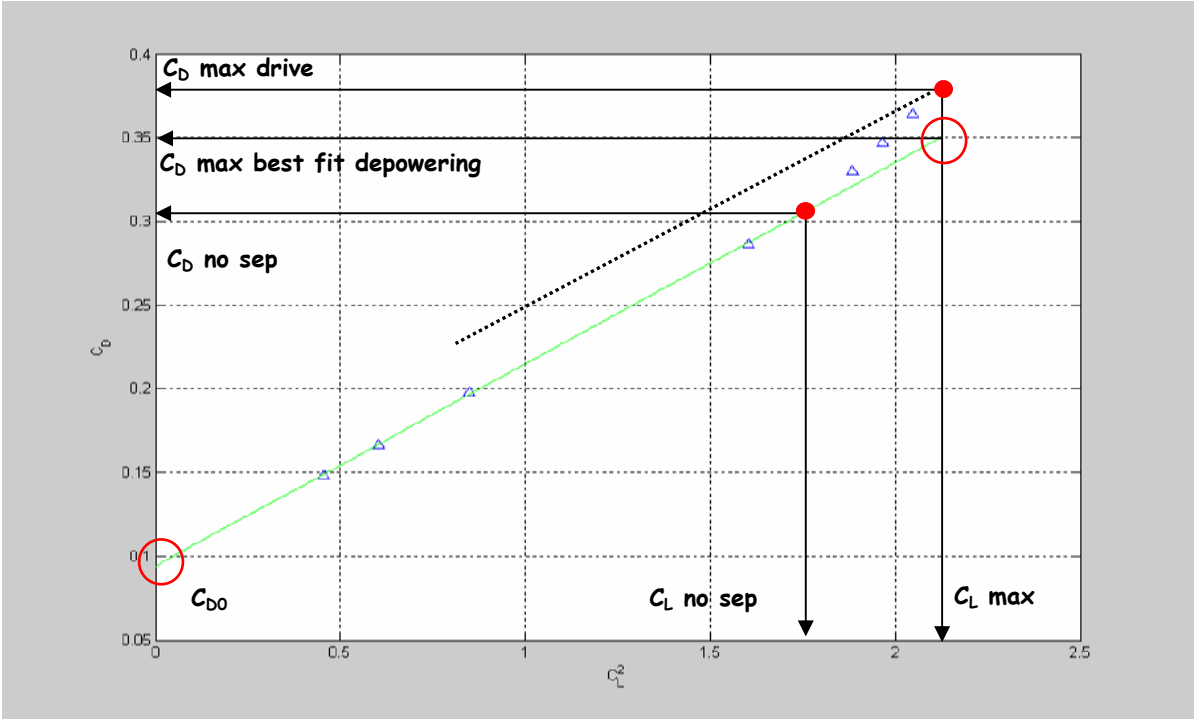

Figure 23

Following the approach proposed in [4], assuming to have a set of realistic depowered trims from the wind tunnel tests this provides the opportunity to develop improved semi-empirical aerodynamic force model.
In particular the basic idea outlined in [4] is that forces and centre of effort height can be modelled as *surfaces* dependent on the apparent wind angle and a newly defined trim parameter named *"Power"*.
Since the main reason for depowering the sails is to reduce the heeling moment, the level of depowering can be quantified by the reduction in heeling moment.
Then the trim parameter "Power" can be defined as the ratio between the heeling moment coefficient C_{Mx} and the maximum heeling moment coefficient C_{Mxmax} for that apparent wind angle.

$$Power = \frac{C_{Mx}(awa)}{C_{Mxmax}(awa)} \tag{22}$$

This way the wind tunnel measurements are assigned at different level of depowering so that the VPP can use the depowered trims by optimising the trim "Power" parameter.
Using the experimental data obtained for each sailplan from wind tunnel tests aerodynamic forces (Lift and Drag) and centre of effort height the basic idea is try to match them using *Bezier Surfaces* which can be evaluated as functions of the *"apparent wind angle"* and *"Power"* parameters.
Using this approach we model the surface as a patch, that is a curve-bounded collection of points whose coordinates are given by continuous two – parameters single valued mathematical functions of the form:

$$x = x(u,w)$$
$$y = y(u,w)$$
$$z = z(u,w)$$

In other words we could define a surface that approximates or approaches the experimental points available from wind tunnel tests.
As well known Bezier surface is defined by means of a characteristic polyhedron which is defined using *(m+1) x (n+1)* control points where *m* and *n* are the Bezier patch degrees.
Bezier started with the principle that any point on a surface must be given by a parametric function if the following form:

$$\underline{p}(u,w) = \sum_{i=0}^{m}\sum_{j=0}^{n} \underline{p}_{ij} B_{i,m}(u) B_{j,n}(w) \qquad (23)$$
$$u,w \in [0,1]$$

where $\underline{p}_{ij}$ is a vector of 3D coordinates of the ij-th control point and $B_{i,m}(u)$ and $B_{j,n}(w)$ are Bernstein polynomials which act as shape function.
In particular with reference to wind tunnel results approximation bicubic Bezier patch have been choosen.
The 3D coordinates of the generic point which belongs to the surface are given by the following relationship:

$$\underline{p}(u,w) = \begin{bmatrix} x_{Sp}(u,w) \\ y_{Sp}(u,w) \\ z_{Sp}(u,w) \end{bmatrix} = \begin{bmatrix} (1-u)^3 & 3u(1-u)^2 & 3u^2(1-u) & u^3 \end{bmatrix} \begin{bmatrix} \underline{p}_{11} & \underline{p}_{12} & \underline{p}_{13} & \underline{p}_{14} \\ \underline{p}_{21} & \underline{p}_{22} & & \\ & & \underline{p}_{33} & \\ \underline{p}_{41} & & & \underline{p}_{44} \end{bmatrix} \begin{bmatrix} (1-w)^3 \\ 3w(1-w)^2 \\ 3w^2(1-w) \\ w^3 \end{bmatrix}$$

The matrix

$$\begin{bmatrix} \underline{p}_{11} & \underline{p}_{12} & \underline{p}_{13} & \underline{p}_{14} \\ \underline{p}_{21} & \underline{p}_{22} & & \\ & & \underline{p}_{33} & \\ \underline{p}_{41} & & & \underline{p}_{44} \end{bmatrix}$$

contains the position vectors of the surface control points which define the vertices of the characteristic polyhedron and thereby the Bezier surface patch (Figure).

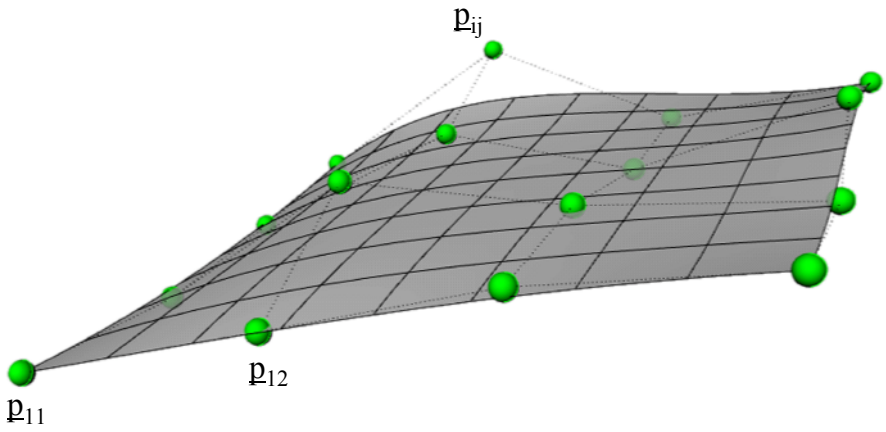

Figure 24

As an example with reference to CL surface the 3D coordinates are:

$$\underline{p}(u,w) = \begin{bmatrix} AWA(u,w) \\ Power(u,w) \\ CL(u,w) \end{bmatrix} \tag{24}$$

and u and w are nondimensional variables ($u,w \in [0,1]$) associated to *AWA* and *Power* values range corresponding to wind tunnel tests performed.
In order to identify the elements of P matrix, i.e the surface control points coordinates, we have to approximate CL values at each AWA as a function of Power values (available from the experimental depowering sequence) by means of a cubic Bezier curve which is a sort of a skeleton of the CL surface patch.
As an example Figure shows the C_L surface and the corresponding control points location with reference to a particular sailplan.

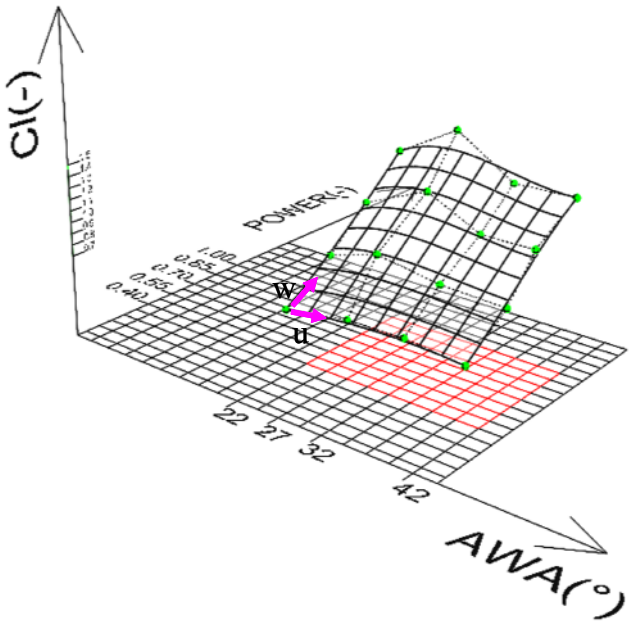

Figure 25

On the basis of the control points location knowledge, for a fixed u and w degree using equation (23) the C_L Bezier patch is univocally determined.
As an example in Figure the Bezier CL surface and experimental measured CL values (red dots) corresponding to different *AWA* and depowering sequence tested are reported.

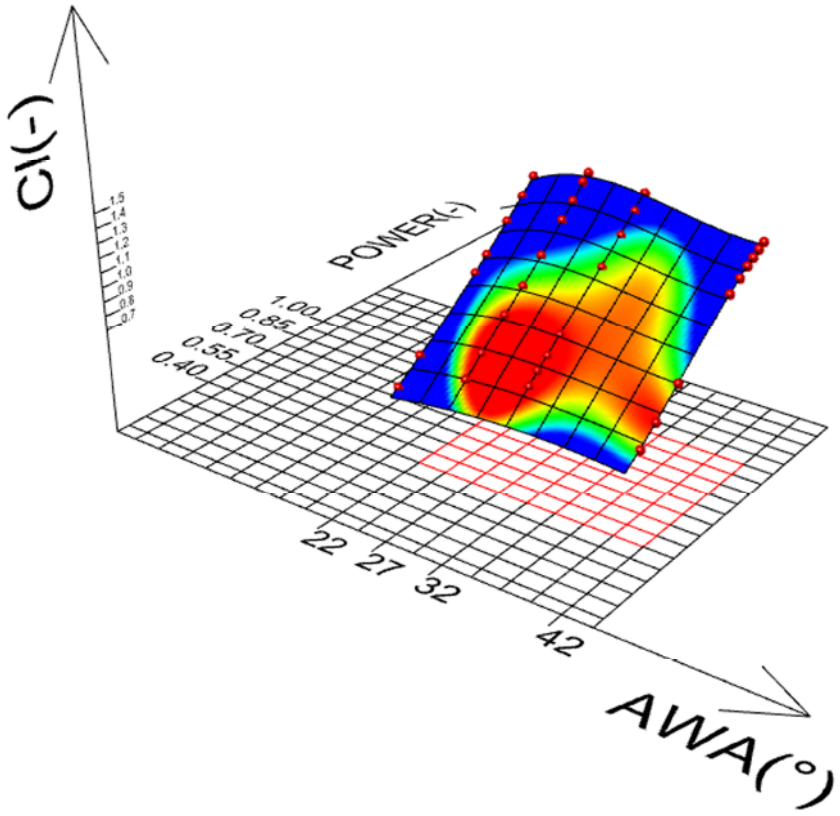

Figure 26

In the same way it's possible to include the dependency of the drag coefficient and centre of effort height from these parameters (Figure – Figure).

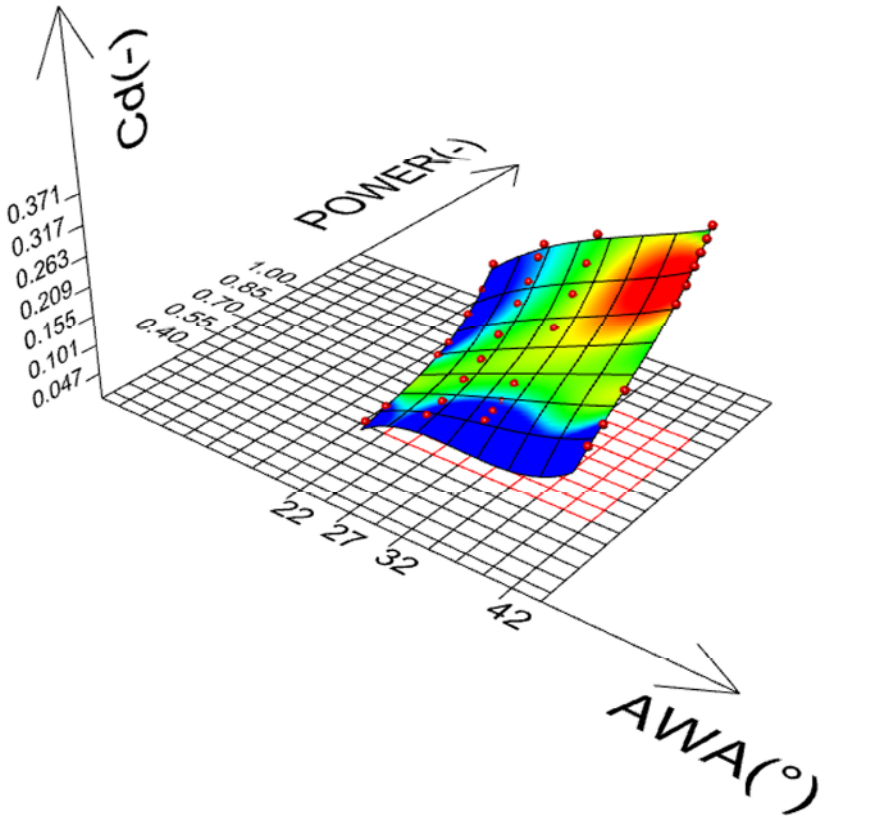

Figure 27

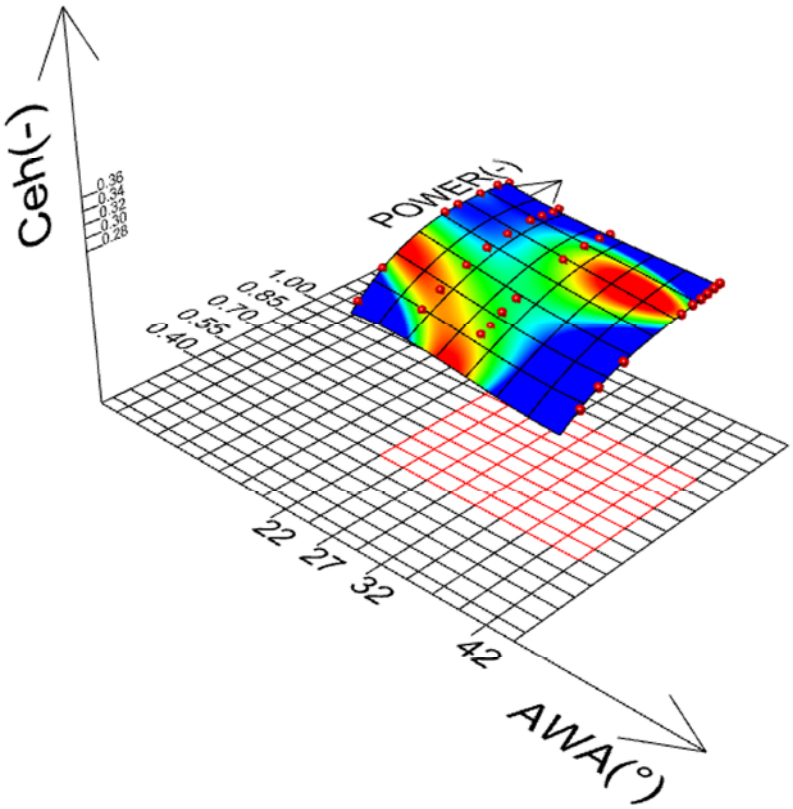

Figure 28

As an example, with reference to a the Main IMS + 100% jib sailplan, in figs 29-30 C_D Bezier surface sections corresponding to 22° and 27° tested apparent wind angles are reported. In the same figures experimental C_D values (dots) are reported as a comparison.

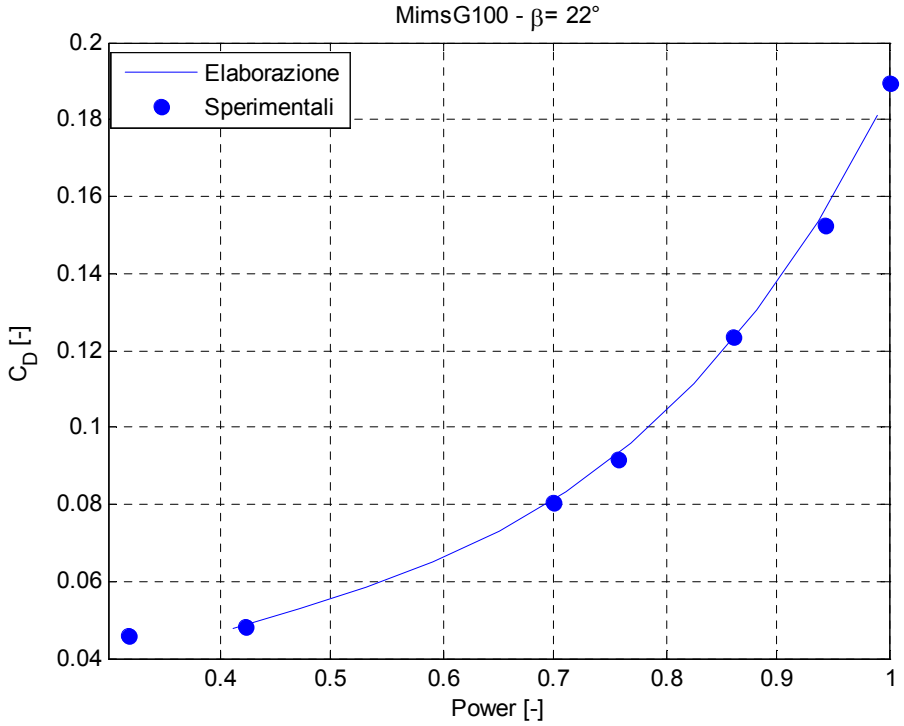

Figure 29

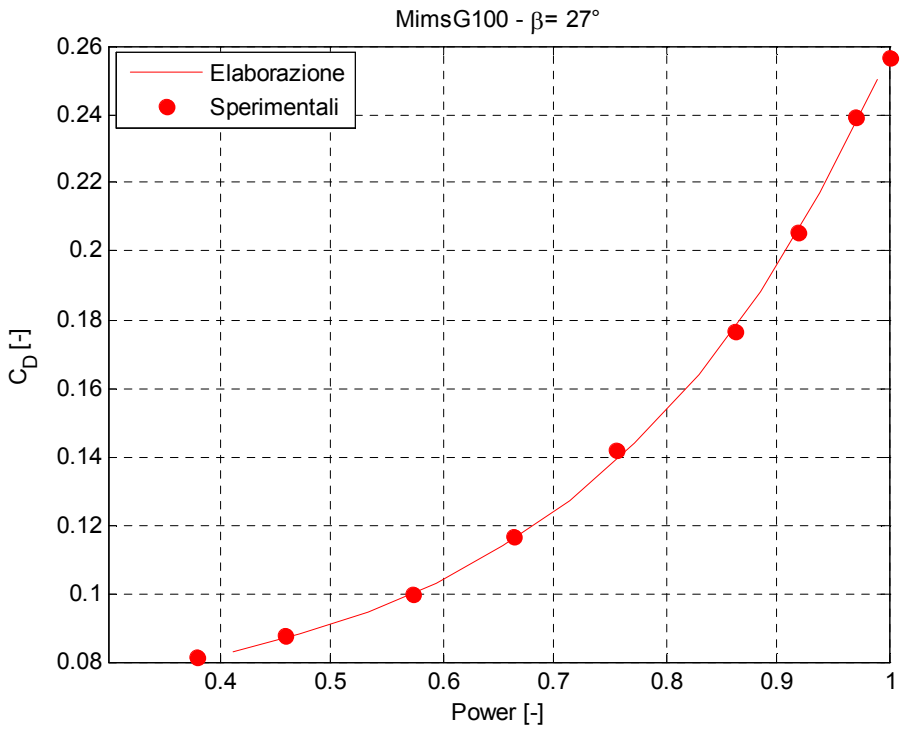

Figure 30

Using the above mentioned approach, for each sailplan tested it is possible to use the relevant C_D C_L and Centre of Effort height surfaces as a function of apparent wind angle *"awa"* and "*Power"* parameter: in particular VPP procedure will take into account these surfaces as sails aerodynamic input data.

VPP solution iterative procedure is not affected by the new aero-model with the main advantage that the proposed formulation is based on *wind tunnel collected results only* without considering any drag superposition effects.

More in details for a given apparent wind angle (AWA) the VPP chooses values of *"Power"* parameter to maximise yacht performance completing the system of equations for the force and moment balance in the same way of the reef and flat concepts.

The main advantage of this formulation is that is based on *wind tunnel collected results only* without considering any drag superposition effects.

3.1. GENERIC SET OF SAILS

In order to include in the aero model the effects of jib overlap and mainsail roach, and in order to take into account that genoa overlap varies, for a given boat, with varying wind speed and the need of de-power, the right way to do could be to attempt to interpolate between the experimental available surfaces data base (which are related to discrete jib overlap and to discrete mainsails roach values).

As an example Figure 31 shows the C_L surface obtained for all the five tested sailplans.

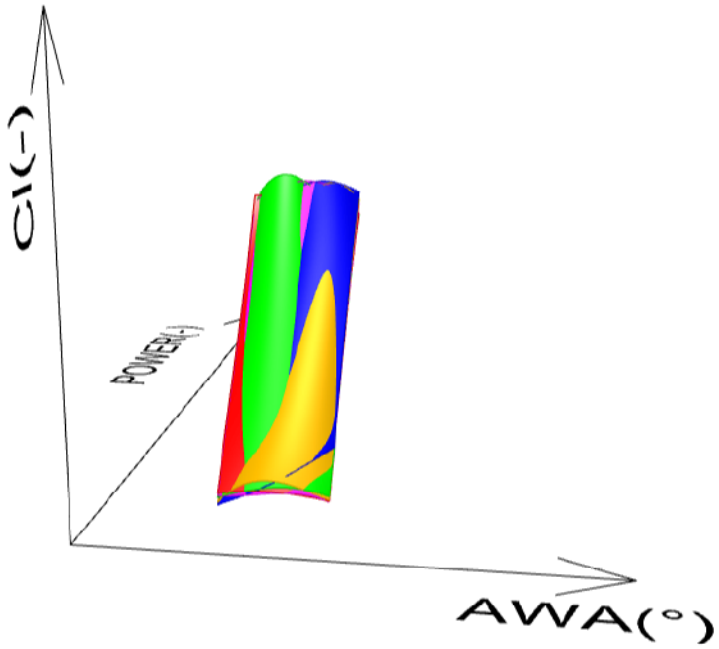

Figure 31

The basic concept has been an investigation of the Bezier Surface control points mathematical dependence on sailplan overlap and roach parameters.
Let's suppose we have an explicit function of the control points 3D coordinates by the sailplan overlap and roach parameters (Figure 32):

$\underline{p}_{ij}(overlap, roach)$

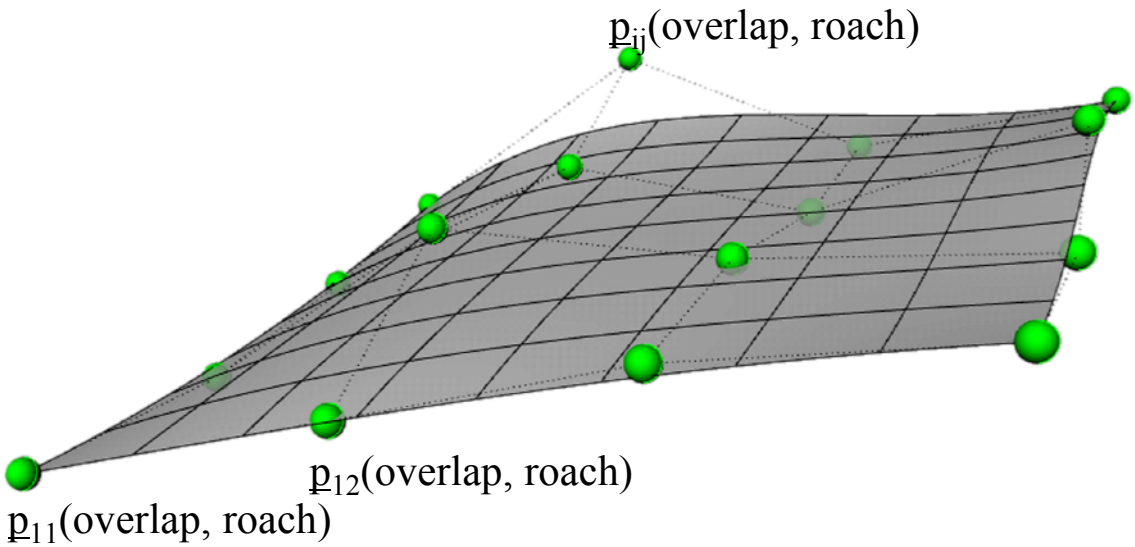

Figure 32

Then it is possible to evaluate the matrix that contains the position vectors of the surface control points which define the vertices of the characteristic polyhedron and thereby the Bezier surface patch relevant to a generic overlap and roach combination:

$$\begin{bmatrix} \underline{p}_{11}(overlap,roach) & \underline{p}_{12}(overlap,roach) & \underline{p}_{1j}(overlap,roach) & \underline{p}_{1N}(overlap,roach) \\ \underline{p}_{21}(overlap,roach) & \underline{p}_{2j}(overlap,roach) & & \\ & & \underline{p}_{ij}(overlap,roach) & \\ \underline{p}_{M1}(overlap,roach) & & & \underline{p}_{MN}(overlap,roach) \end{bmatrix}$$

As an example with reference to CL surface the 3D coordinates are:

$$\underline{p}(u,w)=\begin{bmatrix} AWA(u,w) \\ Power(u,w) \\ CL(u,w) \end{bmatrix}=\begin{bmatrix}(1-u)^3 & 3u(1-u)^2 & 3u^2(1-u) & u^3\end{bmatrix}\begin{bmatrix} \underline{p}_{11}(overlap,roach) & \underline{p}_{12}(overlap,roach) & \underline{p}_{1j}(overlap,roach) & \underline{p}_{1N}(overlap,roach) \\ \underline{p}_{21}(overlap,roach) & \underline{p}_{2j}(overlap,roach) & & \\ & & \underline{p}_{ij}(overlap,roach) & \\ \underline{p}_{M1}(overlap,roach) & & & \underline{p}_{MN}(overlap,roach) \end{bmatrix}\begin{bmatrix}(1-w)^3 \\ 3w(1-w)^2 \\ 3w^2(1-w) \\ w^3\end{bmatrix}$$

and u and w are nondimensional variables ($u,w\in[0,1]$) associated to *AWA* and *Power* values range corresponding to wind tunnel tests performed.
With reference to the tested sailplan, it should be noted that vertices of the characteristic polyhedron aerodynamic coefficients and centre of effort height surfaces are defined by the same apparent wind angles for each sailplan (which means each overlap and roach combination) and by *"Power"* parameter values that are very closer (see Figure 33).

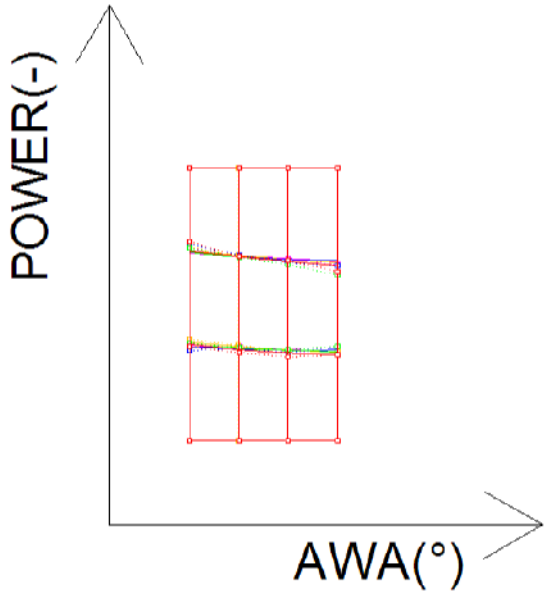

Figure 33

This means we can only consider the surface control points 3rd coordinate variation with respect to overlap and roach parameters combination neglecting the others two coordinates.
In other words we can look for explicit functions between the aerodynamic coefficients and centre of effort height surface 3rd coordinate control points (Zp_{ij}) and overlap and roach parameters:

$$Zp_{ij} = Zp_{ij}(overlap,roach)$$

which can be used during VPP iterations for evaluate the aerodynamic coefficients and centre of effort height for each apparent wind angle and "Power"parameter combination of the generic yacht sailplan.
Considering experimental results available from different sailplan tested (which means for each overlap and roach combination) for each *"apparent wind angle"* and *"Power" parameter*

combination (which define the vertices of the characteristic polyhedron), in order to fit 3rd coordinate control points (Zp_{ij}) measured values, quadratic polynomial surfaces have been choosen:

$$Zp_{ij} = a_0 * overlap^2 + a_1 * roach^2 + a_2 * overlap * roach + a_3 * overlap + a_4 * roach + a_5$$

Coefficients a_0, a_1,….a_5 have been evaluated by means of a least square minimization procedure.

As an example Figure 34, Figure 35, Figure 36 show the surface for the C_D C_L and Ceh values for a fixed couple of apparent wind angle and Power values.
In the same figures experimental points are reported too (dots).

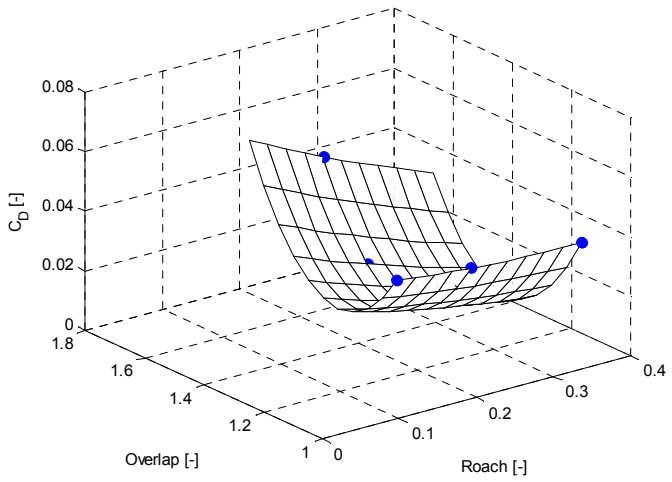

Figure 34

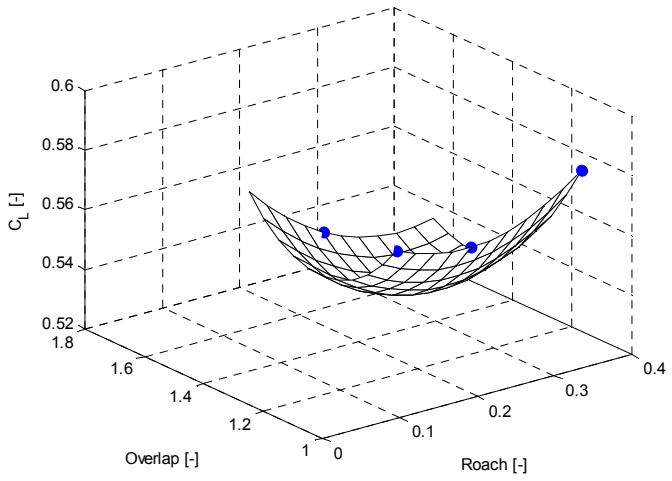

Figure 35

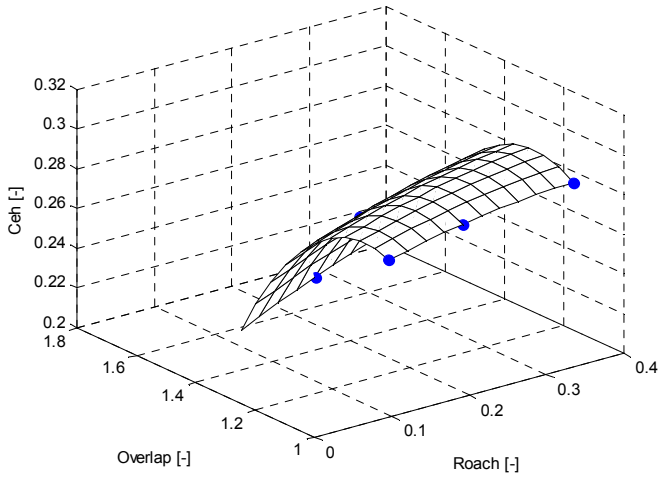

Figure 36

VPP procedure could easily take into account these surfaces as sails aerodynamic input data.
More in details the VPP will try to optimise the boat speed and the *"Power"* parameter concept will be used to complete the system of equations for the force and moment balance in the same way of the reef and flat concepts.
With reference to IMS VPP, the currently used solution iterative procedure should not be affected by the new aero-model with the main advantage that the proposed formulation should be based on *wind tunnel collected results only* without considering any drag superposition effects as the actual IMS aero model does.

4. CONCLUSION

In this paper research activities carried out at Politecnico di Milano Twisted Flow Wind Tunnel with partial funding from the ORC in order to investigate the performance of upwind sails have been summarised. In particular a series of rig planform variations in mainsail roach and jib overlap have been tested. The results of these investigation are used to assist the International Technical Committee (ITC) in upgrade the formulations in the IMS sail aerodynamic model.
Finally some basic ideas to provide a more suitable aero-model for upwind sails as required by IMS VPP to predict the performance of yacht for rating purposes are outlined. The new approach is strongly based on the availability of an experimental data base according to the ITC research program guidelines.
The proposed method is now under ITC analysis and in particular the effects are tested on a sample fleet that the ORC is still committed to handicapping correctly.
The aero model could be improved including also the sailplan fractionality as a geometric parameter affecting the aerodynamics of the sailplan. From this point of view some preliminary results from wind tunnel tests are available and more investigation are planned for the next future.

ACKNOWLEDGEMENTS

This wind tunnel testing have occurred with the financial assistance of the Offshore Racing Congress and the support of Politecnico di Milano CIRIVE Department.
North Sails Italy provided sails and trimming expertise to the program.
There are a number of individuals who contribute to the development of offshore handicapping rules. Authors would like to thank in particular the ITC members and ORC Chairman Bruno Finzi for their continued support.

REFERENCES

1. Kerwin, JE "A velocity Prediction Program for Ocean racing yachts", *Rep 78-11 MIT*, July 1978
2. Fossati, F.& Zasso, A.& Viola I., "Twisted Flow Wind Tunnel Design for Yacht Aerodynamic Studies", *Proc. of the 4th European and African Conference on Wind Engineering*, J. Naprstek & C. Fisher, Prague, 11-15 July, 2005.
3. J. M. C. Campbell, & A. R. Claughton – "Wind Tunnel Testing of Sailing Yacht Rigs" – *13th HISVA symposium* – Amsterdam 1994
4. P. S. Jackson P. Richards & H. Hansen – " An investigation of Aerodynamic Force Modelling for Yacht Sails Using Wind Tunnel" - *Proceedings of the 2nd High Performance Yacht Design Conference* Auckland, 14-16 February, 2006
5. Claughton A, "Development in the IMS VPP Formulations" – *SNAME 14th CSYS,* Annapolis, 1999
6. P. S. Jackson, "Modelling the Aerodynamics of Upwind Sails" – *Journal of Wind Eng. & Ind. Aerodyn.,* vol. 63 , 1996
7. P. S. Jackson, "An improved Upwind Sail Model for VPPs" – *SNAME 15th CSYS,* Annapolis, 2001
8. Teeters J & al., "Changes to Sail Aerodynamics in the IMS Rule", *SNAME 16th CSYS,* Annapolis, 2003
9. Fossati, F.& al., "Wind Tunnel Techniques for Investigation and Optimization of Sailing Yachts Aerodynamics", *Proceedings of the 2nd High Performance Yacht Design Conference* Auckland, 14-16 February, 2006
10. Day, A. "Sail Optimisation for Optimal Speed", *Journal of Wind Eng. & Ind. Aerodyn.,* vol. 63 , 1996
11. Euerle, SE & al, "Toward a rational Upwind Sail Force Model for Vpps" *SNAME 11th CSYS,* Annapolis, 1993
12. Hazen G. " A Model of Sail Aerodynamics for Diverse Rig Types", SNAME 1980